SUPPLEMENTAL INFORMATION

Comparing Photodegradation Model Systems: Measuring Bimolecular Rate Constants Between Photochemically Produced Reactive Intermediates and Organic Contaminants

Luana de Brito Anton[1], Andrea I. Silverman[1], and Jennifer N. Apell[1*]
[1]Civil and Urban Engineering Department, Tandon School of Engineering, New York University, Brooklyn, New York 11201, United States
*Corresponding author: japell@nyu.edu

Table of Contents

Section S1. Materials and Methods

Text S1.1. Stock Solution and Experimental Solution Preparation

All pesticide stock solutions were prepared in acetonitrile (1 g/L, Fisher, HPLC grade). Stock solutions of probe compounds, including furfuryl alcohol (FFA, 10 mM), 2,4,6-trimethylphenol (TMP, 5 mM in 2% acetonitrile), and benzoic acid (5 mM in 2% acetonitrile) were prepared in ultrapure water (≥18.2 MΩ, Millipore Direct-Q 3 UV). Sensitizer stock solutions, including hydrogen peroxide (unstabilized H_2O_2, 100 mM, freshly prepared on the day of experiments), sodium nitrite ($NaNO_2$, 5 mM), zinc porphyrin (ZnP, 50 μM), perinaphthenone (PN, 100 μM), 4-benzoylbenzoic acid (CBBP, 100 μM), benzophenone (BP, 100 μM), and 3'-methoxyacetophenone (3-MAP, 100 μM) were prepared ultrapure water. Phenol was used as a model antioxidant, and 10 mM stock solutions were prepared in ultrapure water.

All working solutions were prepared in ultrapure water. Irradiated solutions contained the pesticide (1 mg/L or one-half the pesticide water solubility when water solubility was <1 mg/L), model sensitizer, probe compound, and phosphate buffer (1 mM at pH=7), except for prothioconazole. Prothioconazole solutions prepared with 1 mM phosphate buffer at pH=5 or pH=9 due to its environmentally relevant pKa of 7.3 (see **Measurement of Prothioconazole pKa** below). Phosphate buffer stock solutions (0.5 M) were prepared by dissolving sodium phosphate dibasic heptahydrate (Na_2HPO_4 x 7 H_2O) in 100 mL of ultrapure water. The pH was then adjusted 5, 7, or 9 as needed by adding phosphoric acid 85% w/w drop-wise. Actinometer solutions of p-nitroanisole (PNA, 10 μM) were prepared in ultrapure water.

For monitoring indirect photodegradation reactions with hydroxyl radicals (•OH), 2 mM H_2O_2 and 100 μM $NaNO_2$ were used as the model sensitizers, and benzoic acid (25 μM) as the probe compound. For singlet oxygen ($^1O_2$) reactions, 1 μM ZnP and 1 μM PN were used as the sensitizers, and 40 μM FFA as the probe compound. Indirect photodegradation reactions with triplet excited states of sensitizers (^{3}sens*) were evaluated using 5 μM 4-CBBP, 10 μM BP, or 5 μM 3-MAP as proxies for the triplet excited states of chromophoric dissolved organic matter (^{3}CDOM*), and 10 μM TMP was used as the probe compound. The kinetic solvent isotope effect (KSIE) was evaluated in $^1O_2$ experiments with 80:20 (by volume) D_2O:H_2O solutions using ZnP as the model sensitizer. Phenol was used as a model antioxidant at 10 μM in ^{3}sens* model systems; this low phenol concentration was used to prevent decreased steady-state concentrations of ^{3}sens* due to reaction with phenol.[1]

Text S1.2. Measurement of Prothioconazole pKa

The pKa of prothioconazole was measured using a previously published protocol.[2] Briefly, prothioconazole solutions were prepared in 1 mM phosphate buffer, and the pH was incrementally adjusted with 0.3 M NaOH or 1 M HCl. The absorbance spectra were measured in a 1 cm pathlength quartz cuvette using a UV-vis spectrophotometer (Cary 60, Agilent). Ratios of absorbance values (A_{244}/A_{265}) at two wavelengths were used to account for dilution; A_{244} represented a peak growing in, and A_{265} represented a wavelength that was unaffected by the pH changes. The data were fitted to **Equation S1.1** to determine the pKa (**Figure S1.1**) where a and b are fitted parameters.

$$\frac{A_{244}}{A_{264}} = \frac{10^{-pH}}{10^{-pKa}+10^{-pH}} \times a + \frac{10^{-pKa}}{10^{-pKa}+10^{-pH}} \times b \qquad \text{(S1.1)}$$

Text S1.3. Calculation of Bimolecular Reaction Rate Constants between ^{3}sens* and TMP

Bimolecular reaction rate constants between ^{3}sens* and TMP ($k_{^3sens*,TMP}$) were calculated using **Equation S1.2**. In solutions with varying concentrations of the sensitizers at pH=7, the TMP log-linear degradation ($k_{obs,TMP}$) was measured and plotted as a function of the calculated steady-state concentration of ^{3}sens* ($[^3sens*]_{ss}$). $[^3sens*]_{ss}$ was calculated following **Equation S1.3**. In **Equation S1.3**, R_f is the rate of formation of ^{3}sens*, R_d is the decay of ^{3}sens*, Φ_{ISC} is the intersystem crossing quantum yields between the singlet and triplet excited states, R_{abs} is the rate of light absorption of ^{3}sens*, k_d is the ^{3}sens* relaxation constant,[3, 4] k_{O_2} is the rate constant for quenching by oxygen,[3, 4] and $[O_2]$ is the concentration of dissolved oxygen. The Φ_{ISC} were assumed to be unity for these three sensitizers based on values reported for structurally similar aromatic ketones.[5, 6] k_d were previously determined using laser flash photolysis.[3, 4] For 3-MAP and BP, k_{O_2} was previously calculated from its corresponding k_d assuming 100% triplet deactivation by oxygen at 255 μM.[3] For 4-CBBP, k_{O_2} was previously determined from the slopes of the linearly fitted data of k_d versus $[O_2]$ using Stern-Volmer approach.[4] In this work, the $[O_2]$ in solution was measured using a dissolved oxygen probe (VWR, sympHony H10D).

The R_{abs} were calculated following **Equation S1.4**, based on the sensitizers' molar absorptivies (ε_λ; **Figure S1.2**), concentration in solution (C; 2-50 μM), the light pathlength (l, 1 cm), and the photon irradiance of UVA bulbs determined using PNA actinometry (I_λ; **Figure S1.3**).

$$k_{^3sens*,TMP} = \frac{k_{obs,TMP}}{[^3sens*]_{ss}} \qquad \text{(S1.2)}$$

$$[^3sens*]_{ss} = \frac{R_f}{R_d} = \frac{\Phi_{ISC} \times R_{abs}}{k_d + k_{O_2} \times [O_2]} \qquad \text{(S1.3)}$$

$$R_{abs} = \sum_\lambda I_\lambda \times (1 - 10^{\varepsilon_\lambda \times C \times l}) \qquad \text{(S1.4)}$$

The values for parameters used are shown in **Table S1.4**, and the $k_{^3sens*,TMP}$ results are reported in **Table 1** in the main text.

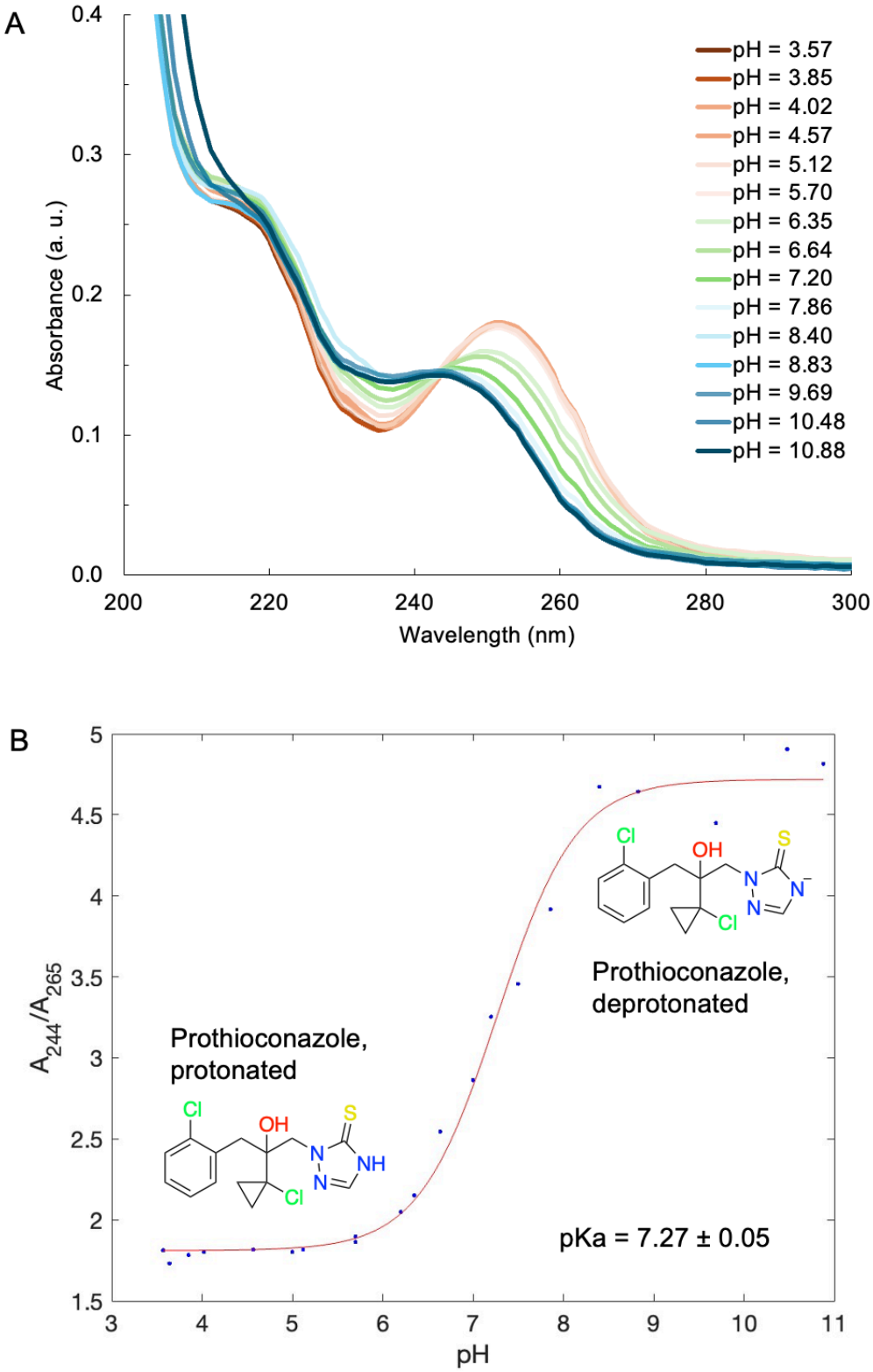

Figure S1.1. (A) Prothioconazole's absorbance spectra at different pH values and (B) its absorbance change as a function of pH to determine the pKa in aqueous solutions. In panel B, the data were fitted using MATLAB curve fitting tool.

Table S1.1. Chemicals used, their purity, and supplier.

Chemical	Purity	Supplier
2,3,6-trimethylphenol	98%	Thermo Fisher Scientific
3'-methoxyacetophenone	98%	Thermo Fisher Scientific
4-benzoylbenzoic acid	99%	Sigma-Aldrich
Acetochlor	≥95%	Sigma-Aldrich
Acetonitrile	HPLC grade	Thermo Fisher Scientific
Alachlor	≥98%	Sigma-Aldrich
Aminopyralid	≥98%	Sigma-Aldrich
Atrazine	≥98%	Sigma-Aldrich
Azoxystrobin	≥98%	Sigma-Aldrich
Benzoic acid	99.5%	Thermo Fisher Scientific
Benzophenone	99%	Sigma-Aldrich
Chlorothalonil	≥98%	Sigma-Aldrich
Chlorpyrifos	≥98%	Sigma-Aldrich
Cyproconazole	99.2%	Thermo Fisher Scientific
Cyprodinil	≥98%	Sigma-Aldrich
Deuterium oxide	99.8 atom % D	Thermo Fisher Scientific
Dicamba	≥98%	Sigma-Aldrich
Difenoconazole	≥95%	Sigma-Aldrich
Fluroxypyr	≥98%	Sigma-Aldrich
Fomesafen	≥98%	Sigma-Aldrich
Furfuryl alcohol	>98%	TCI America
Hydrogen peroxide	30%, unstabilized	Sigma-Aldrich
MCPA	≥98%	Sigma-Aldrich
Mesotrione	≥98%	Sigma-Aldrich
Metconazole	≥98%	Sigma-Aldrich
Metolachlor	≥95%	Sigma-Aldrich
Pendimethalin	≥98%	Sigma-Aldrich
Perinaphthenone	97%	Sigma-Aldrich
Phenol	≥99%	Sigma-Aldrich
Phosphoric acid	≥85% (w/w)	Thermo Fisher Scientific
Picloram	≥98%	Sigma-Aldrich
Picoxystrobin	≥98%	Sigma-Aldrich
p-Nitroanisole	99+%	Sigma-Aldrich
Propiconazole	≥98%	Sigma-Aldrich
Prothioconazole	98.2%	Sigma-Aldrich
Pyraclostrobin	≥98%	Sigma-Aldrich
Pyrimethanil	≥98%	Sigma-Aldrich
Sodium Nitrite	97.9%	Thermo Fisher Scientific
Tebuconazole	>98%	TCI America
Thiobencarb	≥98%	Sigma-Aldrich
Triclopyr	≥98%	Sigma-Aldrich
Trifloxystrobin	≥95%	Sigma-Aldrich
Zn 5,10,15,20-tetra-(4-pyridyl)-21H,23H-porphine tetrakis-(methochloride)	≈85%	American Elements

Table S1.2. Peak height, peak position, and peak width values for the series of Gaussian curves plotted in MATLAB that reconstruct the molar absorptivity (ε_λ) spectra of the model sensitizers and probe compounds. The curves are a result of interpolating multiple ε_λ measurements of the chemicals.[7] The following equation was used to obtain the molar absorptivity values: $\varepsilon_\lambda = \sum_{i=1}^{n}(peak\ height)_i \times exp\left[-\left(\frac{\lambda-(peak\ position)_i}{(peak\ width)_i}\right)^2\right]$.

Sensitizer	curve #1	curve #2	curve #3	curve #4	curve #5	curve #6	curve #7	curve #8	curve #9	curve #10	curve #11	curve #12	curve #13	curve #14
Hydrogen Peroxide (H_2O_2)														
peak height (M^{-1} cm^{-1})	575.3													
peak position (nm)	133.7													
peak width (nm)	66.0													
Sodium Nitrite ($NaNO_2$)														
peak height (M^{-1} cm^{-1})	1816.3	2923.2	679.8	1808.1	1506.6	2342.3	19.7	9.1						
peak position (nm)	209.4	192.4	190.8	202.9	216.1	220.4	356.1	296.9						
peak width (nm)	6.9	9.3	27.4	6.5	8.6	14.1	26.0	56.4						
Zinc Porphyrin (ZnP)														
peak height (M^{-1} cm^{-1})	6521.5	831.5	2348.0	1724.6	6.4	2900.5	8.E+4	1.7E+4	1.1E+4	3506	5575	1.1E+4	2.3E+4	1.5E+4
peak position (nm)	565.5	580.3	554.3	530.7	515.6	605.0	436.7	418.5	324.4	368	237.4	259.7	191.0	216.7
peak width (nm)	13.4	9.3	12.8	39.3	0.03	23.6	17.0	40.8	39.9	18	11.6	16.6	14.9	13.7
Perinaphthenone (PN)														
peak height (M^{-1} cm^{-1})	37858.9	11411.3	15537.3	7250.4	868.6	7780.3	3809.7	8485.0						
peak position (nm)	200.4	223.8	250.8	257.3	321.0	362.2	315.5	404.0						
peak width (nm)	9.3	28.1	9.4	3.0	7.0	22.0	24.7	34.8						
4-carboxybenzophenone (4-CBBP)														
peak height (M^{-1} cm^{-1})	39216.0	4371.7	7898.3	1597.5	9453.4	8624.8	242.1							
peak position (nm)	190.7	207.5	208.7	246.0	275.1	259.8	331.2							
peak width (nm)	13.1	5.0	25.4	11.1	23.8	16.7	24.1							
Benzophenone (BP)														
peak height (M^{-1} cm^{-1})	24174.0	4682.0	5633.3	2693.7	13391	696.4	298.7							
peak position (nm)	198.6	208.0	215.0	254.5	260.9	291.9	321.9							
peak width (nm)	10.4	4.7	11.4	12.9	24.6	12.4	28.5							
3-methoxyacetophenone (3-MAP)														
peak height (M^{-1} cm^{-1})	3.18E+3	1.24E+4	7.92E+3	7.4E+3	304.5	2.0E+3								
peak position (nm)	195.0	208.7	219.9	251.1	287.7	308.8								
peak width (nm)	6.1	17.3	7.4	14.8	10.5	22.2								

Table S1.2. Continued.

Probe Compound	curve #1	curve #2	curve #3	curve #4	curve #5	curve #6	curve #7	curve #8
Furfuryl Alcohol (FFA)								
peak height (M^{-1} cm^{-1})	2875.3	3879.7	2948.3	3509.7	383.3	47.4		
peak position (nm)	200.0	218.6	226.0	210.7	231.3	275.6		
peak width (nm)	19.7	8.3	7.0	10.5	2.7	20.3		
2,4,6-trimethylphenol (TMP)								
peak height (M^{-1} cm^{-1})	259.5	46423.0	6372.6	6116.9	460.2	849.7	205.5	711.2
peak position (nm)	221.7	197.9	219.6	207.2	284.0	271.2	231.9	278.3
peak width (nm)	4.2	6.6	10.8	8.7	4.4	12.5	30.3	8.3
Benzoic acid								
peak height (M^{-1} cm^{-1})	37126.8	2597.3	5757.1	2220.6	5539.3	363.0	111.8	526.6
peak position (nm)	195.4	238.6	228.9	220.8	200.0	281.1	263.2	271.7
peak width (nm)	5.7	6.7	7.5	5.6	39.9	7.0	4.6	7.7

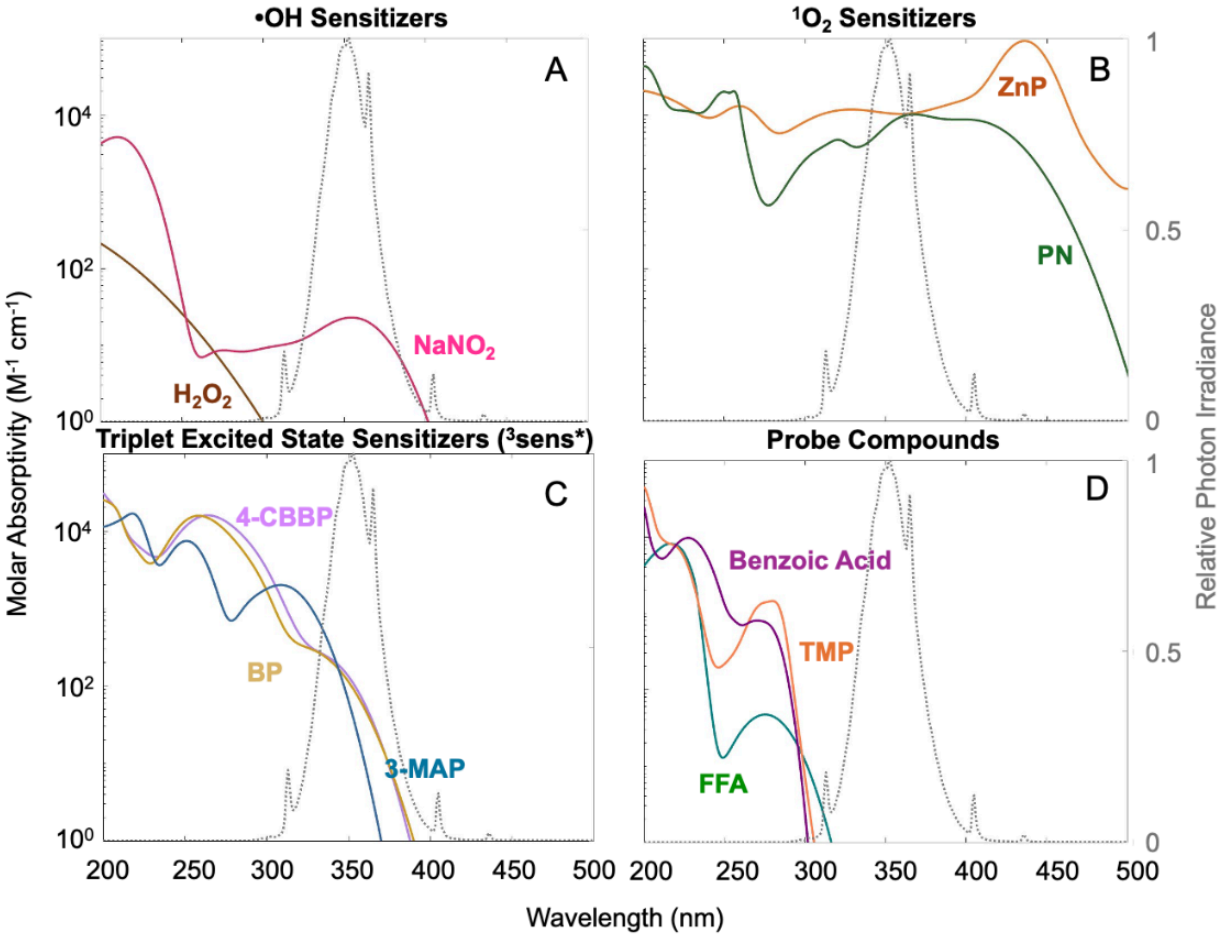

Figure S1.2. Molar absorptivity curves for (A) hydroxyl radical (•OH) sensitizers, (B) singlet oxygen ($^1O_2$) sensitizers, (C) triplet excited states sensitizers (^{3}sens*), and (D) probe compounds. The relative photon irradiance spectrum of the UVA bulbs is represented by the grey dotted curve in each panel (right y-axis). The molar absorptivity curves were obtained from UV-vis spectrophotometer measurements and by fitting a series of Gaussian curves in MATLAB with curve parameters reported in **Table S1.2**.

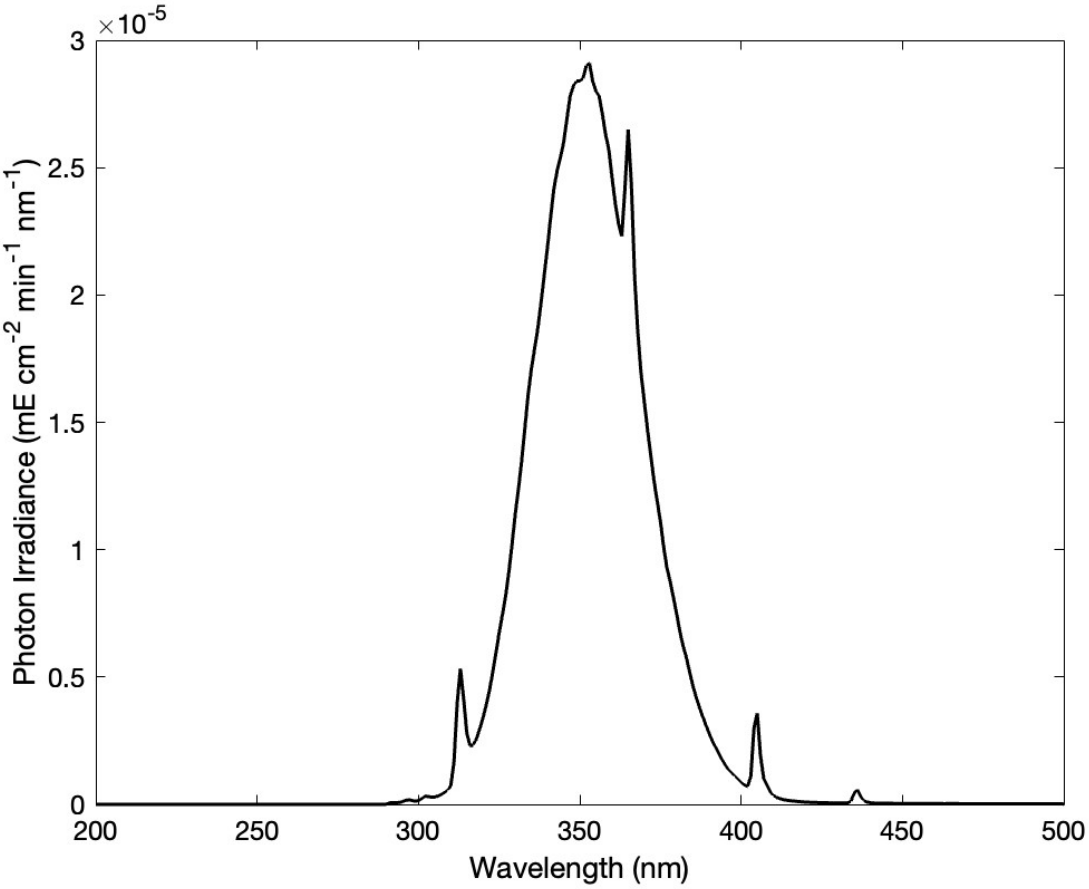

Figure S1.3. Photon irradiance spectrum between 200 to 500 nm of the 8 UVA bulbs placed on the sides of the photoreactor. Spectral irradiance values (W m^{-2} nm^{-1}) were determined using spectroradiometer measurements (Black Comet, StellarNet) and converted to photon irradiances (mE cm^{-2} min^{-1} nm^{-1}) using PNA actinometry.[7] No differences in relative irradiances were observed when the measurements were taken through Pyrex.

Table S1.3. High-performance liquid chromatography parameters for pesticide, probe compound, and actinometer analyses. The parameters include the eluent composition, flow rate, detection wavelength, and retention time for each of compound of interest.

Compound	Eluent A % (Acetonitrile)	Eluent B % (Ultrapure water, 10% acetonitrile)	Eluent C % (10 mM pH=3 phosphate buffer, 10% acetonitrile)	Eluent D % (Methanol)	Flow Rate (mL/ min)	Detection Wavelength (nm)	Retention Time (min)
Acetochlor	80	20	-	-	0.4	230	2.9
Alachlor	80	20	-	-	0.4	230	2.9
Aminopyralid	-	-	100	-	0.5	254	1.9
Atrazine	50	50	-	-	0.6	264	2.1
Azoxystrobin	55	45	-	-	0.6	235	2.4
Chlorothalonil	65	35	-	-	0.6	233	2.4
Chlorpyrifos	80	20	-	-	0.6	229	2.9
Cyproconazole	55	45	-	-	0.6	230	3.6
Cyprodinil	60	40	-	-	0.6	285	3.1
Dicamba	20	-	80	-	0.6	222	3.1
Difenoconazole	70	30	-	-	0.6	247	2.3
Fluroxypyr	40	-	60	-	0.6	211	2.0
Fomesafen	50	-	50	-	0.6	300	3.2
MCPA	40	-	60	-	0.7	230	2.5
Mesotrione	30	-	70	-	0.7	290	3.1
Metconazole	70	30	-	-	0.6	230	2.1
Metolachlor	65	35	-	-	0.6	230	2.4
Pendimethalin	80	20	-	-	0.6	234	2.8
Picloram	-	-	100	-	0.6	254	4.5
Picoxystrobin	70	30	-	-	0.6	215	2.2
Propiconazole	60	40	-	-	0.6	230	2.8
Prothioconazole	60	-	40	-	0.6	260	2.8
Pyraclostrobin	70	30	-	-	0.6	272	2.5
Pyrimethanil	55	45	-	-	0.6	286	2.4
Tebuconazole	60	40	-	-	0.6	230	2.3
Thiobencarb	70	30	-	-	0.6	240	3.0
Triclopyr	-	-	40	60	0.6	254	3.0
Trifloxystrobin	70	30	-	-	0.6	205	2.9
Benzoate	15	-	85	-	0.6	254	3.9
Furfuryl alcohol (FFA)	-	100	-	-	0.6	219	2.3
2,4,6-trimethylphenol (TMP)	40	60	-	-	0.6	220	4.2
p-nitroanisole (PNA)	50	50	-	-	0.6	316	2.2

Table S1.4. Parameters used for calculating the bimolecular reaction rate constants between ^{3}sens* and TMP ($k^{3}_{sens*,TMP}$; **Equations S1.2-S1.4**). More information on parameters and calculations is provided in **Text S1.3**. The $k^{3}_{sens*,TMP}$ results are reported in **Table 1** in the main text.

Model Sensitizer	$k_{obs,TMP}$ (s^{-1})	$[^3sens^*]_{ss}$ (M)	R_{abs} (E s^{-1})	k_d (s^{-1})[3, 4]	k_{O_2} (M^{-1} s^{-1})[3, 4]	$[O_2]$ (M)
4-CBBP						
2 μM	1.09×10^{-4}	2.55×10^{-14}	1.47×10^{-8}			2.89×10^{-4}
5 μM	3.08×10^{-4}	6.20×10^{-14}	3.67×10^{-8}			3.02×10^{-4}
10 μM	5.67×10^{-4}	1.23×10^{-13}	7.33×10^{-8}			3.03×10^{-4}
20 μM	1.10×10^{-3}	2.44×10^{-13}	1.46×10^{-7}	2.00×10^{5}	1.30×10^{9}	3.05×10^{-4}
30 μM	1.32×10^{-3}	3.31×10^{-13}	2.18×10^{-7}			3.08×10^{-4}
40 μM	1.72×10^{-3}	4.78×10^{-13}	2.89×10^{-7}			3.10×10^{-4}
50 μM	2.20×10^{-3}	5.91×10^{-13}	3.59×10^{-7}			3.14×10^{-4}
BP						
2 μM	7.52×10^{-5}	8.29×10^{-15}	1.18×10^{-8}			3.09×10^{-4}
5 μM	1.79×10^{-4}	2.10×10^{-14}	2.94×10^{-8}			3.05×10^{-4}
10 μM	3.36×10^{-4}	4.18×10^{-14}	5.88×10^{-8}			3.06×10^{-4}
20 μM	5.71×10^{-4}	8.20×10^{-14}	1.17×10^{-7}	6.73×10^{5}	2.60×10^{9}	2.91×10^{-4}
30 μM	7.80×10^{-4}	1.19×10^{-13}	1.75×10^{-7}			2.82×10^{-4}
40 μM	1.10×10^{-3}	1.59×10^{-13}	2.33×10^{-7}			2.82×10^{-4}
50 μM	1.34×10^{-3}	1.97×10^{-13}	2.90×10^{-7}			2.88×10^{-4}
3-MAP						
2 μM	6.03×10^{-5}	1.03×10^{-14}	1.88×10^{-8}			3.01×10^{-4}
5 μM	1.78×10^{-4}	2.52×10^{-14}	4.68×10^{-8}			3.09×10^{-4}
10 μM	2.47×10^{-4}	4.96×10^{-14}	9.30×10^{-8}			3.14×10^{-4}
20 μM	3.90×10^{-4}	9.94×10^{-14}	1.84×10^{-7}	8.38×10^{5}	3.30×109	3.07×10^{-4}
30 μM	9.24×10^{-4}	1.46×10^{-13}	2.73×10^{-7}			3.13×10^{-4}
40 μM	1.14×10^{-3}	1.94×10^{-13}	3.60×10^{-7}			3.09×10^{-4}
50 μM	1.38×10^{-3}	2.36×10^{-13}	4.46×10^{-7}			3.18×10^{-4}

Section S2. •OH Model Systems: Hydrogen Peroxide (H_2O_2) and Nitrite (NO_2^-)

Text S2.1. Evaluating the selectivity of benzoic acid as the probe compound in H_2O_2 and NO_2^- model systems

The selectivity of benzoic acid as the probe compound was evaluated from the log-linear degradation of benzoic acid relative to that of PNA for each pesticide in experiments using H_2O_2 and NO_2^- as sensitizers. The average slope and the standard deviation (SD) was 0.96±0.21, with relative standard deviations (RSD) of 22% in the H_2O_2 model system, and 0.20±0.02 (RSD=12%) in the NO_2^- model system.

In both model systems, pesticides with slopes outside the range defined by the average ± one SD include chlorothalonil, pendimethalin, and trifloxystrobin. Solutions for these three pesticides, and chlorpyrifos, were the only that contained <0.1% acetonitrile. The lower volume of acetonitrile compared to ≈0.1% for the other pesticides was achieved by adding a smaller volume of the stock solution (prepared in acetonitrile), due to their lower water solubilities, to ensure working solutions would have a concentration that was approximately half of the water solubility of the pesticide.

In addition to these pesticides, protonated and deprotonated prothioconazole exhibited slopes outside the average ± one SD in the NO_2^- model system only. In this case, the photoproduction of •OH when using NO_2^- is known to be pH-dependent.[8] In contrast, •OH production from H_2O_2 photolysis was reported to be independent of pH values (from 2-7).[9]

As discussed in the **•OH Model Systems: Hydrogen Peroxide (H_2O_2) and Nitrite (NO_2^-)** section in the main text, pesticides with significant relative percent differences (RPDs) between $k_{\bullet OH}$ in H_2O_2 and NO_2^- model systems, with values ranging from 31 to 149%, included alachlor, atrazine, chlorothalonil, cyprodinil, mesotrione, prothioconazole, pyraclostrobin, and trifloxystrobin (**Table S2.1**). However, of these eight pesticides, five had slopes within the average ± one SD calculated based on the results in each system, as shown in **Figure S2.3**. Therefore, benzoic acid as the probe compound is not suspected the cause of discrepancies in measured $k_{\bullet OH}$ across the two model systems. Additionally, the consistency in slopes observed for most of the investigated pesticides indicates that benzoic acid had a strong selectivity for •OH.

Table S2.1. Bimolecular rate constants (in M^{-1} s^{-1}) between hydroxyl radicals (•OH) and the pesticide ($k_{•OH}$) obtained using hydrogen peroxide (H_2O_2) and nitrite (NO_2^-) as model sensitizers. Reported $k_{•OH}$ values in the literature, along with the sensitizer and probe compounds used, are included for comparison. Plots of $k_{•OH}$ measured in this work and those reported in the literature are also shown in **Figure S2.2**.

Pesticide	Bimolecular Rate Constant $k_{•OH,pesticide}$ (M^{-1} s^{-1})		*% Difference*	Literature			
	Hydrogen Peroxide (H_2O_2)	Sodium Nitrite ($NaNO_2$)		$k_{•OH,pesticide}$ (M^{-1} s^{-1})	Sensitizer	Probe Compound	Reference
Acetochlor	$(6.99 \pm 0.10) \times 10^9$	$(5.38 \pm 0.08) \times 10^9$	26%	$(6.3\pm0.5)\times10^9$	O_3/H_2O_2	p-CBA$^{\mu}$	Acero et al. (2003)[10]
				$(7.5\pm2.0)\times10^9$	NO_3^-	Butyl chloride	Brekken & Brezonik (1998)[11]
Alachlor	$(4.86 \pm 0.13) \times 10^9$	$(6.73 \pm 0.19) \times 10^9$	32%	2.2×10^9	H_2O_2	n.a.	Song et al. (2008)[12]
				5.0×10^9	O_3/H_2O_2	Atrazine	De Laat et al. (1996)[13]
				5.4×10^9	H_2O_2	p-CBA$^{\mu}$	Sanches et al. (2010)[14]
				6.1×10^9	TiO_2	p-CBA$^{\mu}$	Sanches et al. (2010)[14]
				7.0×10^9	Photo-Fenton reaction (Fe^{2+}/H_2O_2)	Acetophenone	Haag & Yao (1992)[15]
Aminopyralid	$(3.49 \pm 0.06) \times 10^9$	n.a.$^{\delta}$	-	n.a.			
Atrazine	$(2.35 \pm 0.04) \times 10^9$	$(1.58 \pm 0.03) \times 10^9$	39%	8.2×10^8	H_2O_2	PNDA	Mabury & Crosby (1996)[16]
				1.7×10^9	O_3/H_2O_2	Chlorobenzene	Chramostra et al. (1993)[17]
				$(2.1\pm0.1)\times10^9$	H_2O_2	n.a.	De Laat et al. (1995)[18]
				2.2×10^9	Radiolysis, saturated N_2O	n.a.	Azenha et al. (2003)[19]
				$(2.5\pm0.2)\times10^9$	Fenton reaction	Benzoic acid	Balci et al. (2009)[20]
				$(2.6\pm0.4)\times10^9$	Photo-Fenton reaction (Fe^{2+}/H_2O_2)	Acetophenone	Haag & Yao (1992)[15]
				3.0×10^9	O_3/H_2O_2 Radiolysis, saturated N_2O	Acetophenone n.a.	Acero et al. (2000)[21] Tauber & Von Sonntag (2000)[22]
				7.3×10^9	H_2O_2	p-CBA$^{\mu}$	Sanches et al. (2010)[14]
				1.8×10^{10}	H_2O_2	Phenol	Beltran et al. (1993)[23]
				3.5×10^{10}	TiO_2	p-CBA$^{\mu}$	Sanches et al. (2010)[14]

Table S2.1. Continued.

Pesticide	Bimolecular Rate Constant $k_{•OH,pesticide}$ (M^{-1} s^{-1})		*% Difference*	Literature			
	Hydrogen Peroxide (H_2O_2)	Sodium Nitrite ($NaNO_2$)		$k_{•OH,pesticide}$ (M^{-1} s^{-1})	Sensitizer	Probe Compound	Reference
Azoxystrobin	$(7.70 \pm 0.18) \times 10^9$	$(6.93 \pm 0.13) \times 10^9$	11%			n.a.	
Chlorothalonil	$(2.31 \pm 0.05) \times 10^{10}$	$(1.06 \pm 0.02) \times 10^{11}$	128%	1.4×10^9	H_2O_2	Acetophenone	Armbrust (2000)[24]
Chlorpyrifos	$(6.20 \pm 0.08) \times 10^9$	$(7.03 \pm 0.16) \times 10^9$	13%	4.2×10^9	H_2O_2	Acetophenone	Armbrust (2000)[24]
				$(4.9 \pm 0.1) \times 10^9$	H_2O_2	Nitrobenzene	Wu et al. (2010)[25]
Cyproconazole	$(4.06 \pm 0.08) \times 10^9$	$(4.14 \pm 0.06) \times 10^9$	2%			n.a.	
Cyprodinil	$(8.50 \pm 0.10) \times 10^9$	$(1.44 \pm 0.02) \times 10^{10}$	52%			n.a.	
Dicamba	$(3.20 \pm 0.04) \times 10^9$	$(3.25 \pm 0.08) \times 10^9$	2%	1.33×10^9	H_2O_2	Acetophenone	Armbrust (2000)[24]
Difenoconazole	$(6.51 \pm 0.20) \times 10^9$	$(7.38 \pm 0.20) \times 10^9$	13%			n.a.	
Fluroxypyr	$(5.02 \pm 0.03) \times 10^9$	$(5.06 \pm 0.02) \times 10^9$	1%	$(2.15 \pm 0.75) \times 10^{10}$	H_2O_2	Nitrobenzene	Bhat et al. (2022)[26]
Fomesafen	$(3.15 \pm 0.01) \times 10^9$	$(3.01 \pm 0.03) \times 10^9$	5%			n.a.	
MCPA	$(6.65 \pm 0.02) \times 10^9$	$(6.78 \pm 0.07) \times 10^9$	2%	1.7×10^9	H_2O_2	PNDA	Mabury & Crosby (1996)[16]
				3.6×10^9	H_2O_2	2,4-D[θ]	Fdil et al. (2003)[27]
				6.6×10^9	O_3/H_2O_2	p-CBA[μ]	Benitez et al. (2004)[28]
				$(3.85 \pm 0.23) \times 10^{10}$	Fenton reaction	2-HBA[ρ]	Housari et al. (2011)[29]
Mesotrione	$(4.74 \pm 0.09) \times 10^9$	$(1.65 \pm 0.02) \times 10^9$	97%	1.0×10^9	Electro-Fenton reaction	4-HBA[ψ]	Murati et al. (2012)[30]
				$(8.8 \pm 0.2) \times 10^9$	Fenton reaction	p-CBA[μ]	Bensalah et al. (2011)[31]
Metconazole	$(6.69 \pm 0.13) \times 10^9$	$(6.70 \pm 0.08) \times 10^9$	0.1%			n.a.	
Metolachlor	$(6.35 \pm 0.12) \times 10^9$	$(5.35 \pm 0.17) \times 10^9$	17%	5.1×10^9	O_3/H_2O_2	Atrazine	De Laat et al. (1996)[13]
				$(6.1 \pm 0.6) \times 10^9$	H_2O_2	Phenol	Huntscha et al. (2008)[32]
				$(6.7 \pm 0.4) \times 10^9$	O_3/H_2O_2	p-CBA[μ]	Acero et al. (2003)[10]
				$(9.1 \pm 0.2) \times 10^9$	H_2O_2	Nitrobenzene	Wu et al. (2007)[25]
Pendimethalin	$(6.72 \pm 0.08) \times 10^9$	$(5.80 \pm 0.12) \times 10^9$	15%			n.a.	
Picloram	$(3.37 \pm 0.03) \times 10^9$	$(3.69 \pm 0.03) \times 10^9$	9%	1.30×10^9	H_2O_2	PNDA	Mabury & Crosby (1996)[16]
				3.40×10^9	Photo-Fenton reaction (Fe^{2+}/H_2O_2)	Acetophenone	Haag & Yao (1992)[15]

Table S2.1. Continued.

Pesticide	Bimolecular Rate Constant $k_{\bullet OH,pesticide}$ (M^{-1} s^{-1})		*% Difference*	Literature			
	Hydrogen Peroxide (H_2O_2)	Sodium Nitrite ($NaNO_2$)		$k_{\bullet OH,pesticide}$ (M^{-1} s^{-1})	Sensitizer	Probe Compound	Reference
Picoxystrobin	$(6.27 \pm 0.12) \times 10^9$	$(6.51 \pm 0.12) \times 10^9$	4%			n.a.	
Propiconazole	$(5.32 \pm 0.08) \times 10^9$	$(5.73 \pm 0.17) \times 10^9$	7%			n.a.	
Prothioconazole (protonated, pH 5)	$(6.48 \pm 0.15) \times 10^{10}$	$(1.00 \pm 0.02) \times 10^{10}$	149%			n.a.	
Prothioconazole (deprotonated, pH 9)	n.a.[α]	$(2.99 \pm 0.07) \times 10^{10}$	-			n.a.	
Pyraclostrobin	$(7.67 \pm 0.27) \times 10^9$	$(1.27 \pm 0.05) \times 10^{10}$	49%			n.a.	
Pyrimethanil	$(8.49 \pm 0.05) \times 10^9$	$(1.01 \pm 0.02) \times 10^{10}$	17%			n.a.	
Tebuconazole	$(5.79 \pm 0.05) \times 10^9$	$(5.99 \pm 0.14) \times 10^9$	3%	$(1.2 \pm 0.3) \times 10^{10}$	H_2O_2	2-propanol	Carena et al. (2022)[33]
Thiobencarb	$(6.43 \pm 0.14) \times 10^9$	$(6.51 \pm 0.20) \times 10^9$	1%	1.89×10^9	H_2O_2	Acetophenone	Armbrust (2000)[24]
Triclopyr	$(1.47 \pm 0.07) \times 10^9$	n.a.[δ]	-	1.19×10^9	H_2O_2	Acetophenone	Armbrust (2000)[24]
Trifloxystrobin	$(5.88 \pm 0.13) \times 10^9$	$(8.00 \pm 0.09) \times 10^9$	31%			n.a.	

[δ] *Only direct photolysis was observed.*
[α] *The pesticide degraded in dark controls.*
[μ] *p-CBA: p-chlorobenzoic acid*
[θ] *2,4-D: 2,4-dichlorophenoxyacetic acid*
[ρ] *2-HBA: 2-hydroxybenzoic acid*
[ψ] *4-HBA: 4-hydroxybenzoic acid*

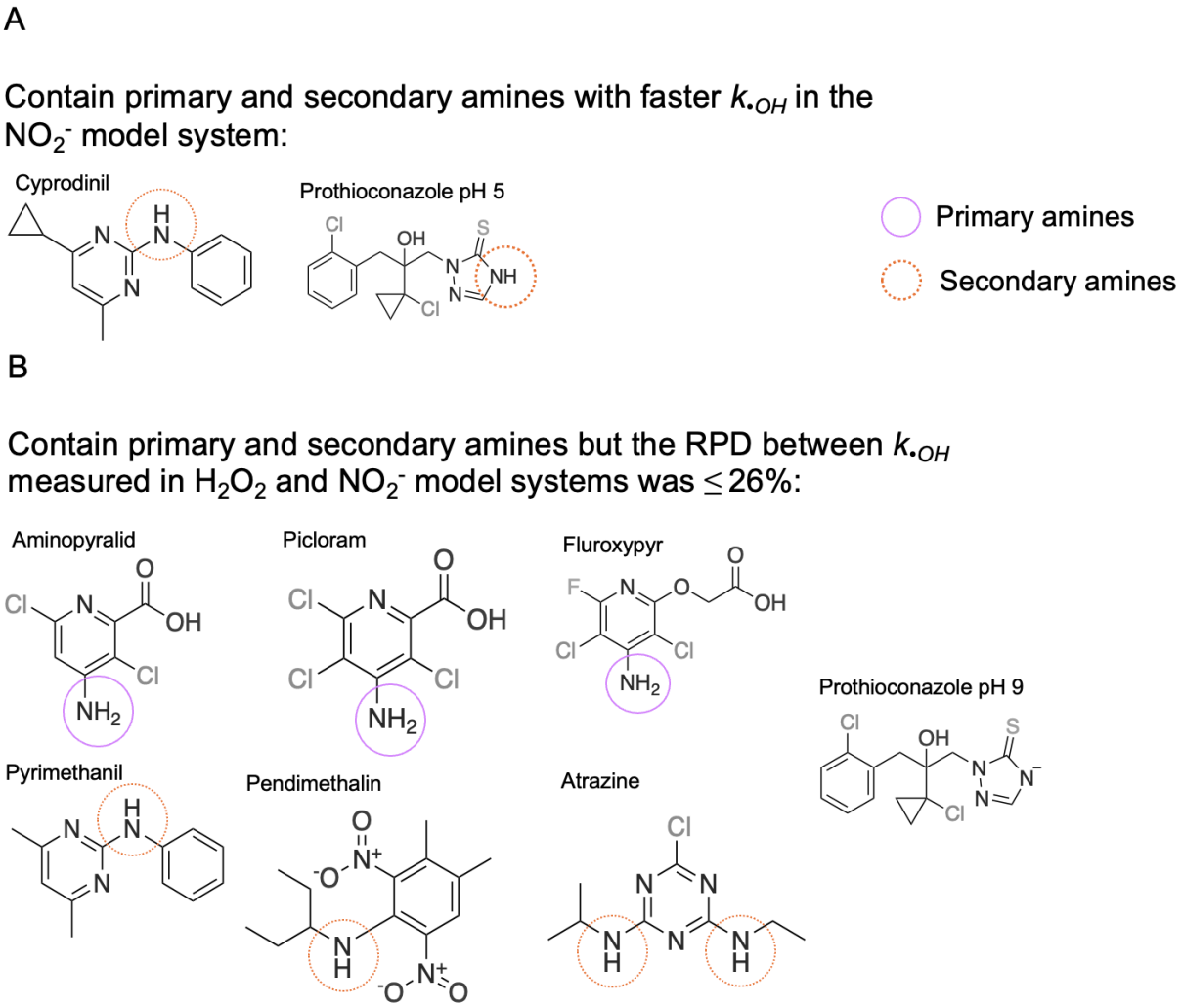

Figure S2.1. Structures of pesticides investigated that contain primary or secondary amines. Pesticides in panel (A) had faster $k_{\bullet OH}$ as measured in the NO_2^- model system than in the H_2O_2 system, and in (B) had $k_{\bullet OH}$ measured in the two model systems with relative percent differences (RPDs) ≤26% (**Table S2.1**).

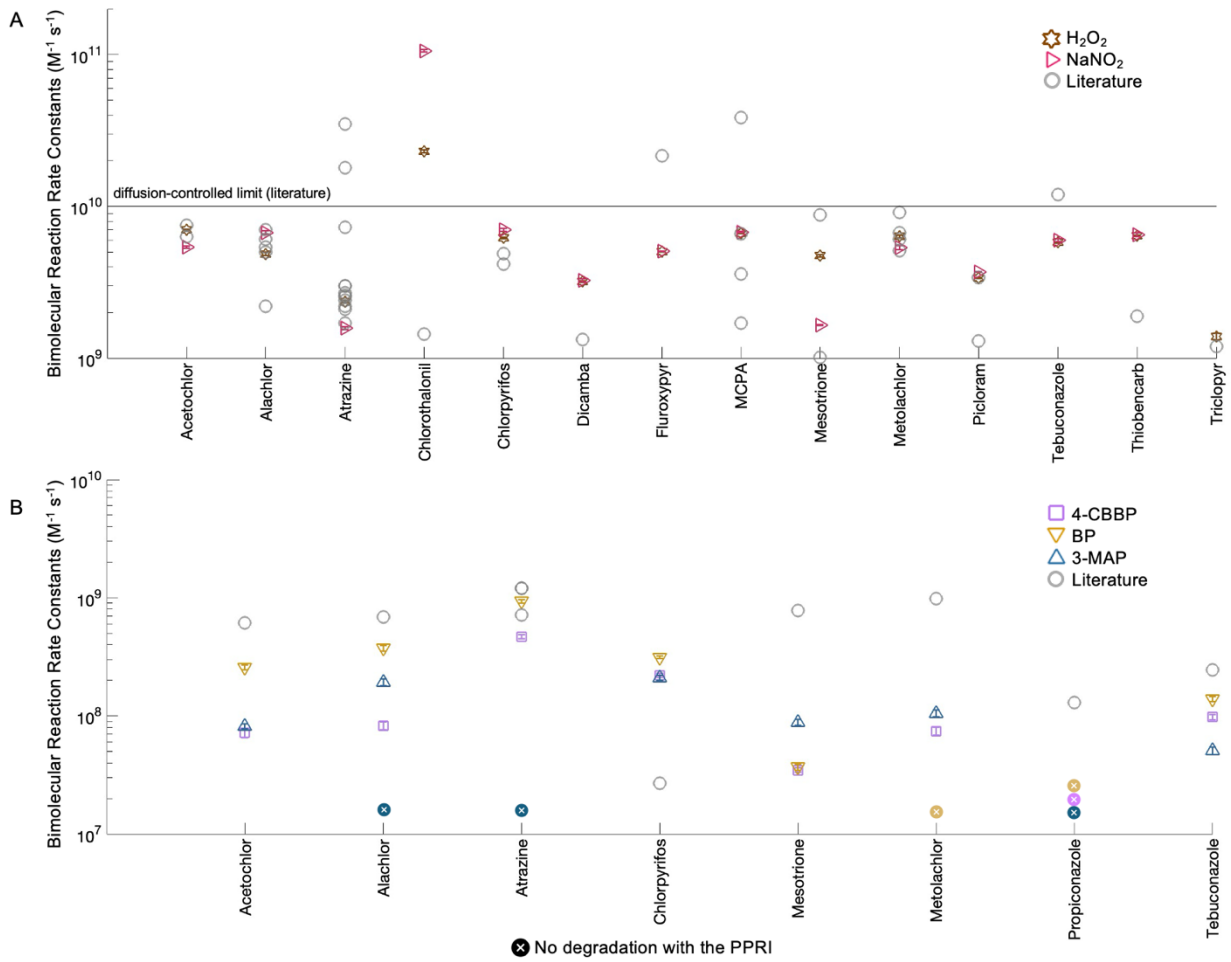

Figure S2.2. Bimolecular reaction rate constants (in M^{-1} s^{-1}) between the pesticides and (A) •OH or (B) ^{3}sens* measured in the model systems compared to values reported in the literature, which are represented as grey circles. For numerical values, sensitizers used, and their respective references see **Tables S2.1** and **S4.1**.

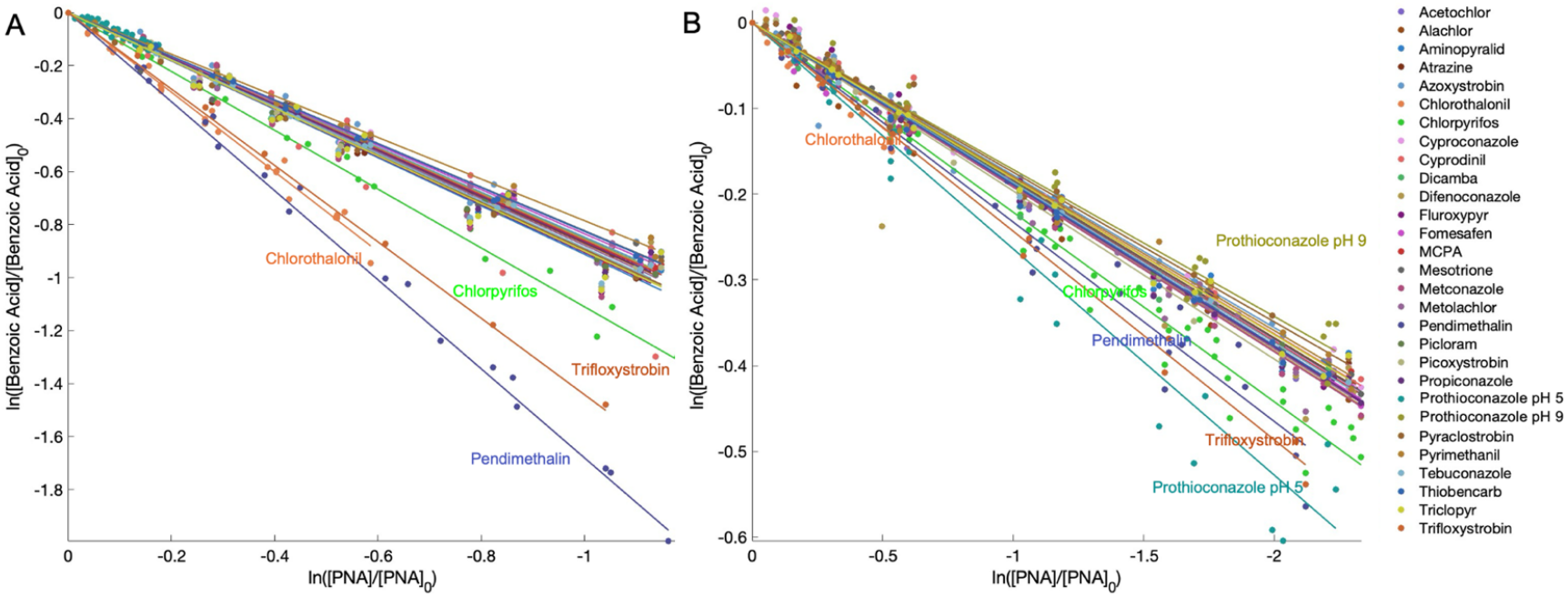

Figure S2.3. Degradation of benzoic acid relative to that of PNA for each pesticide in experiments using (A) H_2O_2 and (B) NO_2^- as the sensitizers. Pesticides that had slopes outside the range defined by the mean ± one standard deviation are indicated by their names (see **Text S2.1** for details).

Section S3. $^1O_2$ Model Systems: Perinaphthenone (PN), Zinc Porphyrin (ZnP), and D_2O Kinetic Solvent Isotope Effect

Text S3.1. Kinetic Solvent Isotope Effect Calculations

In $^1O_2$ model systems, comparative analysis of the kinetic solvent isotope effect (KSIE) enabled calculating the fraction of $^1O_2$-mediated reactions ($f_{^1O_2}$) following **Equation S3.1**:[34]

$$f_{^1O_2} = \frac{KSIE_{observed}}{KSIE_{predicted}} \qquad \text{(S3.1)}$$

Where $KSIE_{predicted}$ was calculated following **Equation S3.2**[34] and $KSIE_{observed}$ following **Equation S3.3**:

$$KSIE_{predicted} = [-0.942 \times (D_2O\ fraction) + 0.988]^{-1} \qquad \text{(S3.2)}$$

$$KSIE_{observed} = \frac{\left[\frac{\ln\left(\frac{[pesticide]}{[pesticide]_0}\right)}{\ln\left(\frac{[PNA]}{[PNA]_0}\right)}\right]_{ZnP,H_2O}}{\left[\frac{\ln\left(\frac{[pesticide]}{[pesticide]_0}\right)}{\ln\left(\frac{[PNA]}{[PNA]_0}\right)}\right]_{ZnP,80:20\ D_2O:H_2O}} \qquad \text{(S3.3)}$$

Direct photolysis control experiments were also performed in 80:20 D_2O:H_2O, but pesticides had similar degradation rates as those measured in H_2O-only solutions. The log-linear decay of the pesticides as a function of that of PNA in $^1O_2$ model systems is shown in **Figure S3.2**, and calculated $KSIE_{observed}$ and $f_{^1O_2}$ are reported in **Table S3.1**.

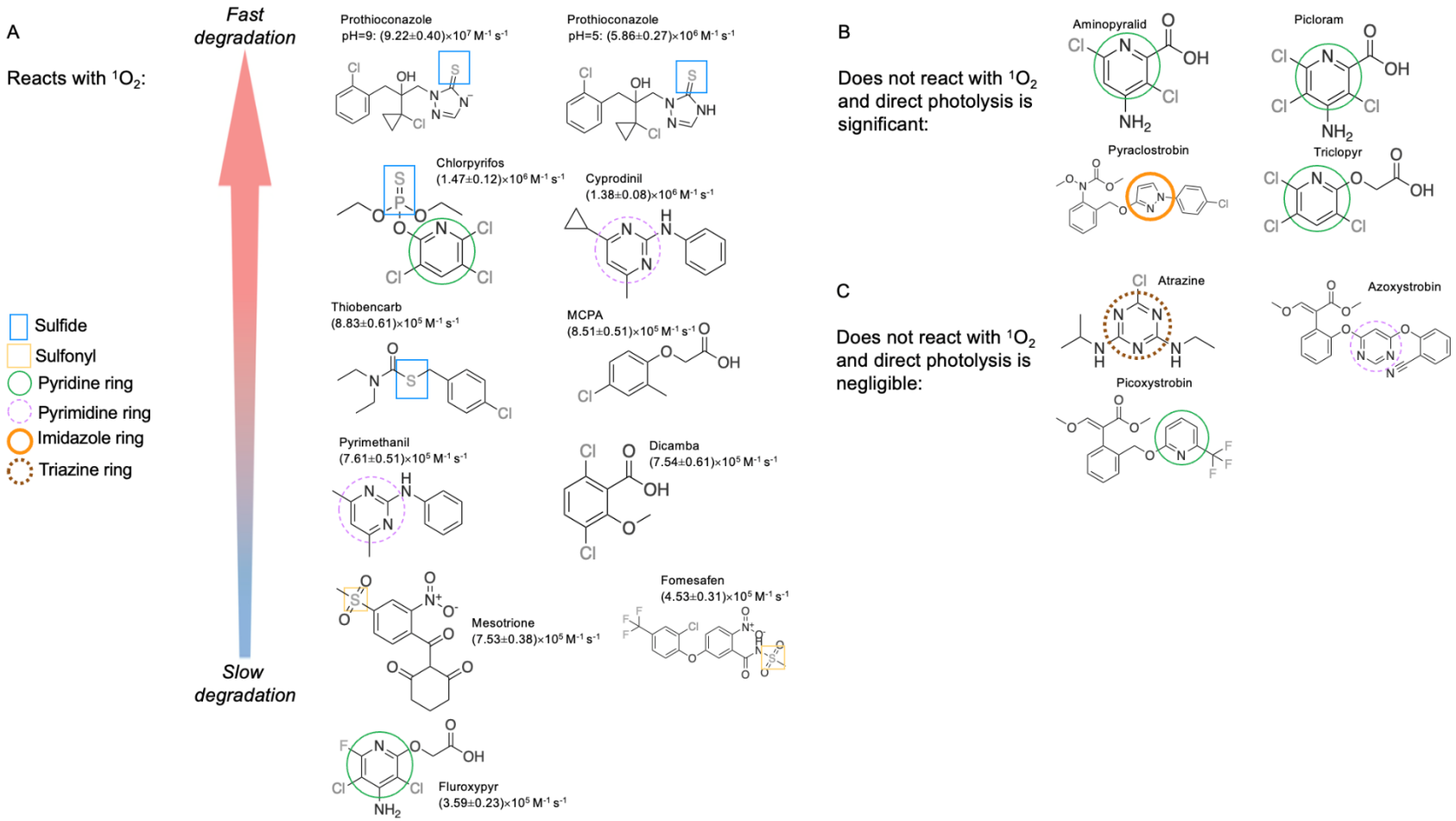

Figure S3.1. Structures of pesticides that (A) reacted with $^1O_2$, (B) did not react with $^1O_2$ and had significant direct photolysis decay, and (C) did not react with $^1O_2$ and direct photolysis was negligible. Functional groups are highlighted (see legend).

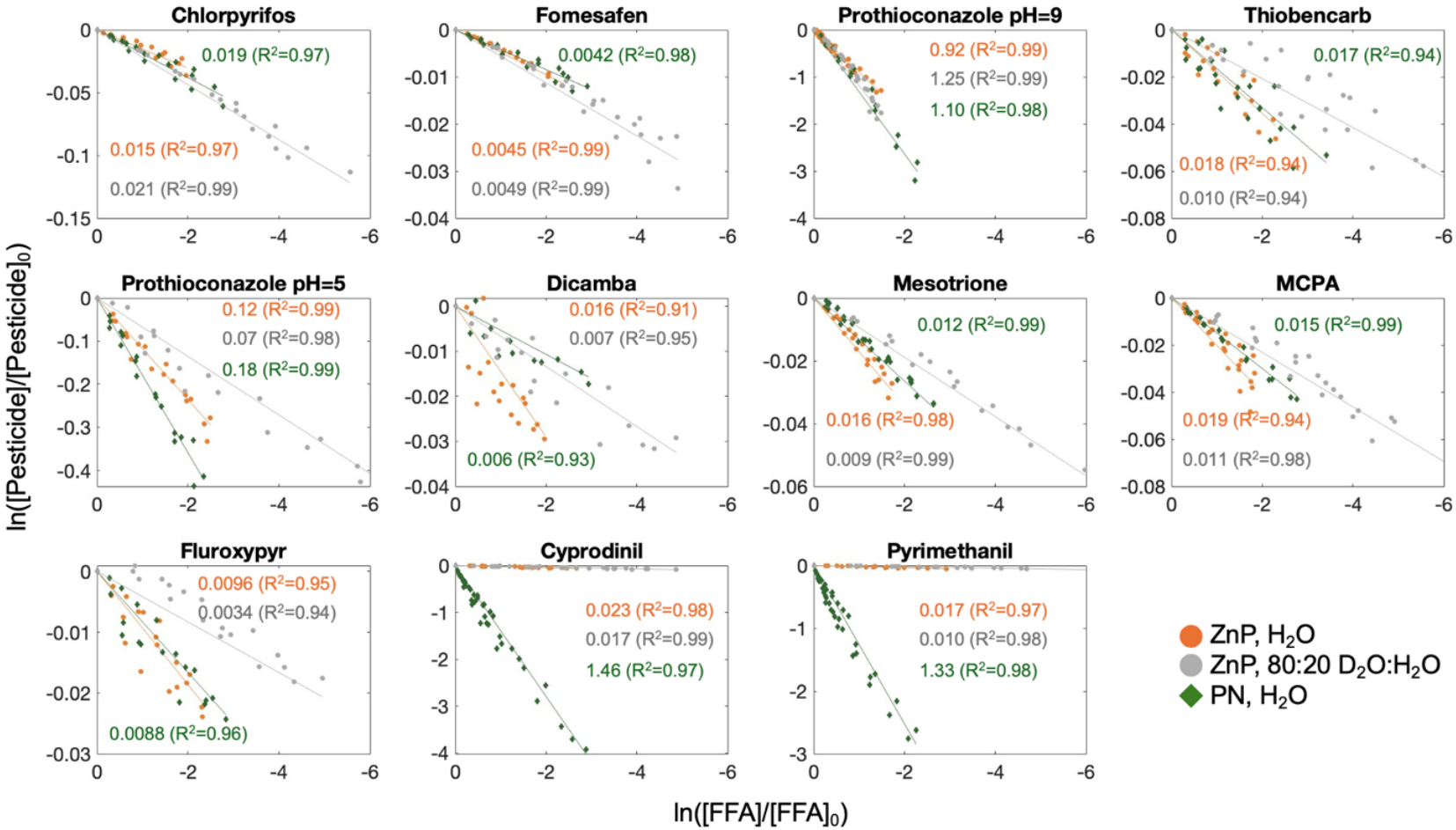

Figure S3.2. Degradation of pesticides plotted against the degradation of the probe compound (FFA) for the 10 pesticides that reacted with $^1O_2$. The slopes of the curves and the coefficient of determination (R^2) are provided. The degradation of pesticides plotted against the degradation of the actinometer (PNA) is provided in **Figure S3.3**.

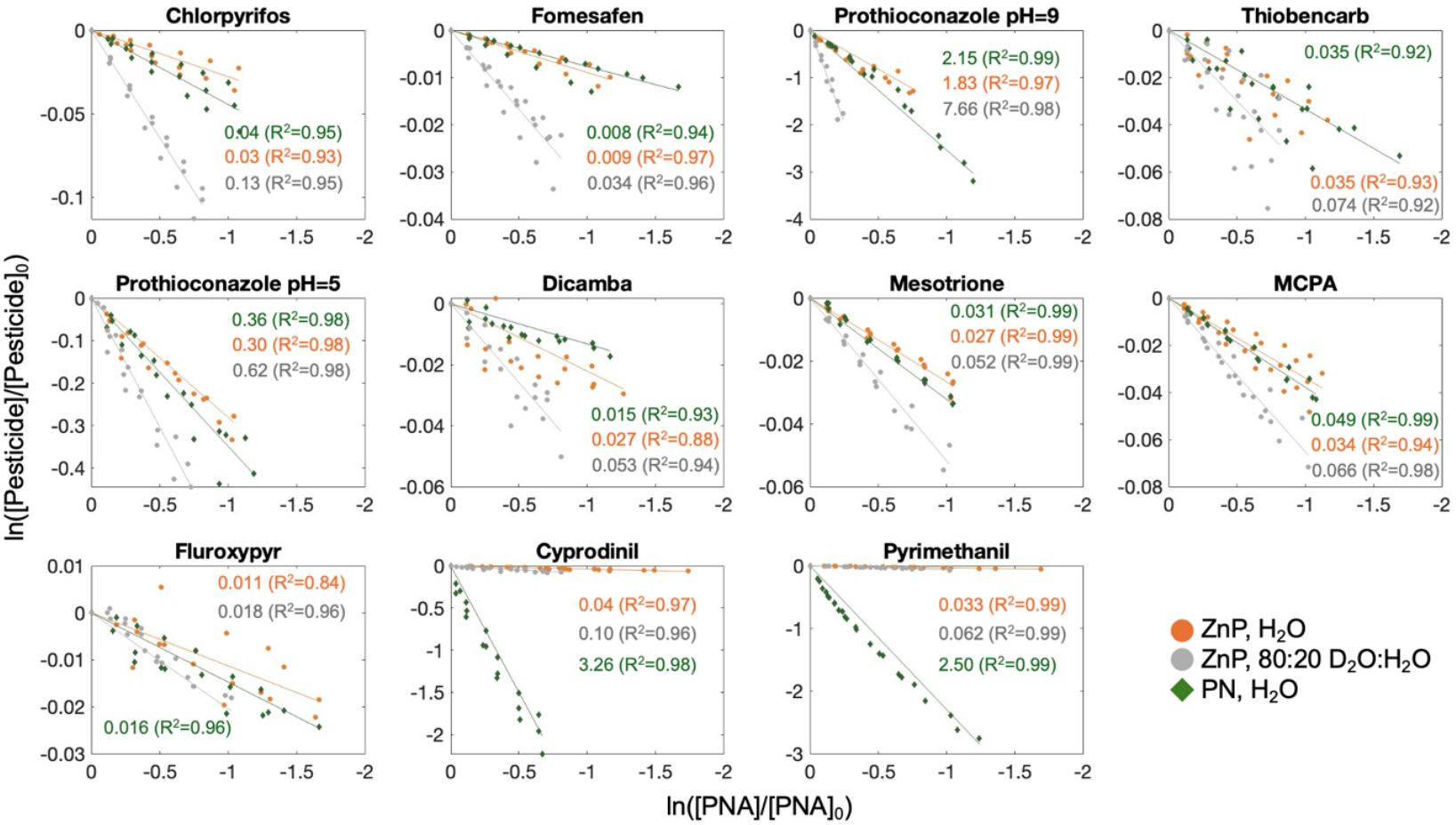

Figure S3.3. Degradation of the pesticides plotted against the degradation of PNA for the 10 pesticides that reacted with $^1O_2$. The slopes of the curves and the coefficient of determination (R^2) are provided.

Table S3.1. Bimolecular rate constants between $^1O_2$ and the pesticide ($k_{^1O_2}$ in M^{-1} s^{-1}) obtained using ZnP and PN as model sensitizers. To quantify the contribution of $^1O_2$-only reactions, the kinetic solvent isotope effect (KSIE) was used (**Text S3.1**). The fraction of $^1O_2$ reactions ($f_{^1O_2}$; **Equation S3.1**) was obtained from observed and predicted KSIE ratios (**Equations S3.2-S3.3**). $KSIE_{predicted}$ was equal to 4.3. The $k_{^1O_2}$ measured in ZnP/H_2O systems were multiplied by $f_{^1O_2}$ to account for $^1O_2$ reactions and exclude the contribution of reactions with ^{3}ZnP* to the pesticide observed degradation. The $k_{^1O_2}$ calculated based on data obtained in PN/H_2O model systems were only reported when similar values were obtained in both model systems, consistent with their similar degradation in all three model systems tested (**Figure S3.2**). When available, $k_{^1O_2}$ reported in the literature were included for comparison to the values calculated in this work.

Pesticide	Observed Reaction Rate Constant, k_{obs} (M^{-1} s^{-1}) In ZnP/D_2O:H_2O	$KSIE_{observed}$	$f_{^1O_2}$	Bimolecular Rate Constant, $k_{^1O_2}$ (M^{-1} s^{-1})		
				ZnP × $f_{^1O_2}$	PN	Literature
Chlorpyrifos	$(2.15 \pm 0.13) \times 10^6$	4.4	1.04≈1.00	$(1.47 \pm 0.12) \times 10^6$	$(1.87 \pm 0.13) \times 10^6$	n.a.
Cyprodinil	$(1.71 \pm 0.11) \times 10^6$	2.5	0.59	$(1.38 \pm 0.08) \times 10^6$	n.a.$^\beta$	n.a.
Dicamba	$(7.18 \pm 0.46) \times 10^5$	2.0	0.47	$(7.55 \pm 0.61) \times 10^5$	n.a.$^\beta$	n.a.
Fluroxypyr	$(3.44 \pm 0.23) \times 10^5$	1.6	0.37	$(3.59 \pm 0.23) \times 10^5$	n.a.$^\beta$	n.a.
Fomesafen	$(5.37 \pm 0.32) \times 10^5$	3.8	0.89≈1.00	$(4.53 \pm 0.31) \times 10^5$	$(4.16 \pm 0.32) \times 10^5$	n.a.
MCPA	$(1.11 \pm 0.06) \times 10^6$	1.9	0.45	$(8.52 \pm 0.51) \times 10^5$	n.a.$^\beta$	n.a.
Mesotrione	$(9.08 \pm 0.48) \times 10^5$	2.0	0.46	$(7.54 \pm 0.38) \times 10^5$	n.a.$^\beta$	$(5.3\pm1.3)\times10^5$ $^\Psi$, ref. 35 $(6.7\pm0.3)\times10^5$ $^\Psi$, ref. 36
Prothioconazole (pH=5)	$(7.13 \pm 0.35) \times 10^6$	2.1	0.48	$(5.86 \pm 0.27) \times 10^6$	n.a.$^\beta$	n.a.
Prothioconazole (pH=9)	$(1.10 \pm 0.05) \times 10^8$	4.2	0.98≈1.00	$(9.22 \pm 0.40) \times 10^7$	$(1.25 \pm 0.06) \times 10^8$	n.a.
Pyrimethanil	$(1.01 \pm 0.05) \times 10^6$	1.9	0.44	$(7.61 \pm 0.51) \times 10^5$	n.a.$^\beta$	n.a.
Thiobencarb	$(9.74 \pm 0.62) \times 10^5$	2.1	0.50	$(8.83 \pm 0.61) \times 10^5$	n.a.$^\beta$	n.a.

$^\beta$ *Confounding reactions with both $^1O_2$ and ^{3}PN**

$^\Psi$ *Using Rose Bengal (171 kJ mol^{-1}, 1.23 V_{SHE})[37] as the sensitizer and FFA as probe compound, irradiation at 546 nm*

Section S4. ^{3}CDOM* Model Systems: benzophenone (BP), 4-carboxybenzophenone (4-CBBP), and 3-methoxyacetophenone (3-MAP)

Text S4.1. Calculation of bimolecular reaction rate constants of pesticides that had degradation affected by the probe compound in the model systems

When observed degradation rates in control experiments (i.e., sensitizer and pesticide only) differed from those measured including the probe, the bimolecular rate constants between the pesticides and the ^{3}sens* (k^{3}_{sens*}) were calculated from the degradation rates of the pesticide and the probe in separate solutions following **Equation S4.1**. Control experimental solutions contained either the pesticide and the sensitizer or the probe and the sensitizer, in contrast to the model system experiments included all three.

$$k_{^3sens*} = \frac{\frac{\left[\ln\left(\frac{[pesticide]_t}{[pesticide]_0}\right)\right]_{control}}{\ln\left(\frac{[PNA]_t}{[PNA]_0}\right)}}{\frac{\left[\ln\left(\frac{[probe]_t}{[probe]_0}\right)\right]_{control}}{\ln\left(\frac{[PNA]_t}{[PNA]_0}\right)}} \times k_{^3sens*,TMP} \qquad \text{(S4.1)}$$

In **Equation S4.**1, [pesticide] and [probe] represent the concentration of the pesticide and probe compound at each time point (represented with the subscript t) and the subscript 0 represents the initial concentration, and $k^{3}_{sens*,TMP}$ is the bimolecular rate constant between the ^{3}sens* and TMP (**Table 1** in the main text). The degradation of the pesticide or probe relative to that of PNA was obtained using linear regression to determine the best fit slope.

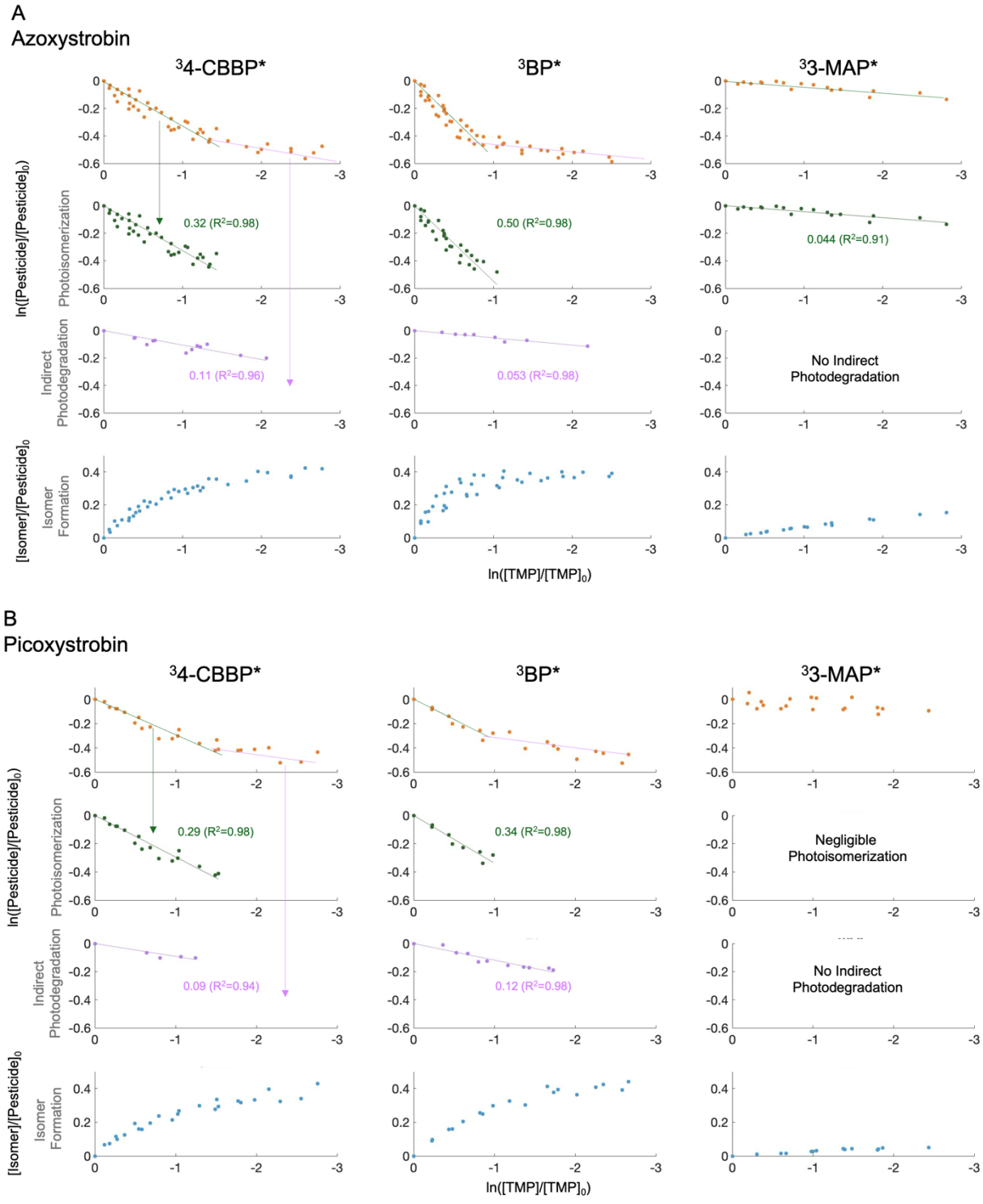
A
Azoxystrobin
^{3}4-CBBP*
^{3}BP*
^{3}3-MAP*
ln([Pesticide]/[Pesticide]$_0$)
Photoisomerization
0.32 (R^2=0.98)
0.50 (R^2=0.98)
0.044 (R^2=0.91)
Indirect Photodegradation
0.11 (R^2=0.96)
0.053 (R^2=0.98)
No Indirect Photodegradation
[Isomer]/[Pesticide]$_0$
Isomer Formation
ln([TMP]/[TMP]$_0$)
B
Picoxystrobin
^{3}4-CBBP*
^{3}BP*
^{3}3-MAP*
ln([Pesticide]/[Pesticide]$_0$)
Photoisomerization
0.29 (R^2=0.98)
0.34 (R^2=0.98)
Negligible Photoisomerization
Indirect Photodegradation
0.09 (R^2=0.94)
0.12 (R^2=0.98)
No Indirect Photodegradation
[Isomer]/[Pesticide]$_0$
Isomer Formation
ln([TMP]/[TMP]$_0$)

Figure S4.1. Continued.

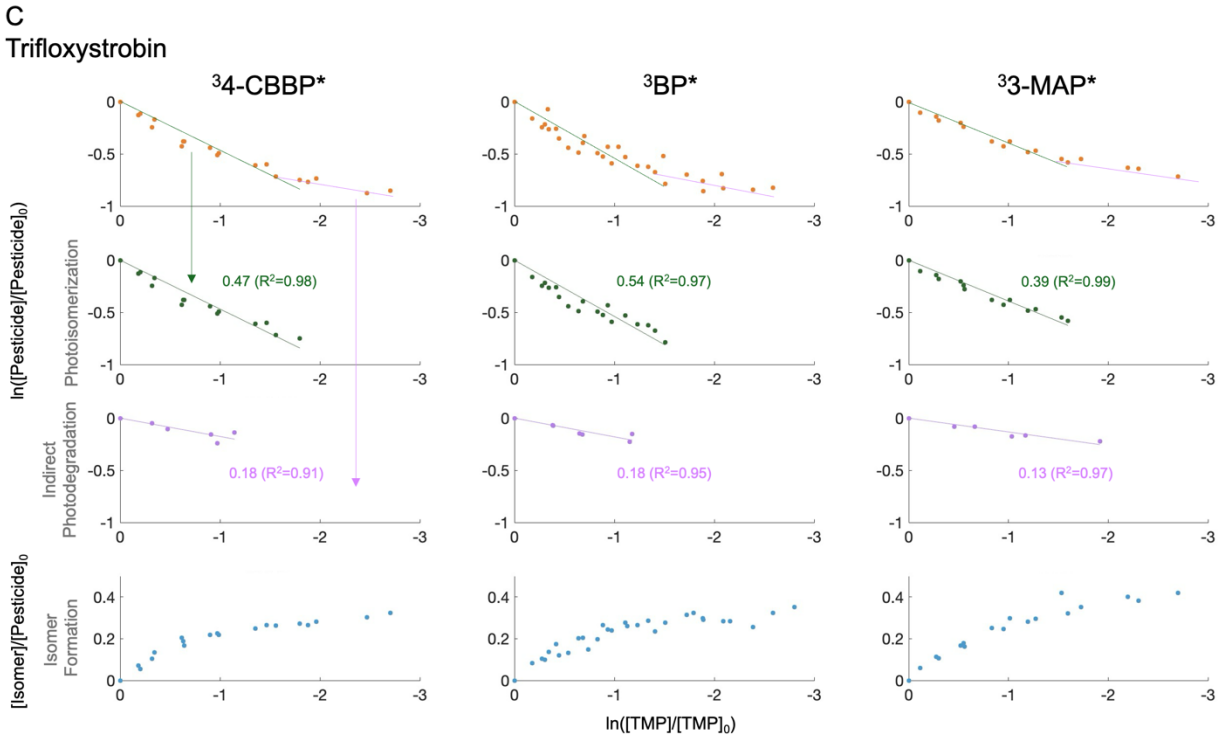

Figure S4.1. Degradation of the pesticide or formation of the isomer (relative to the pesticide initial concentration) plotted against TMP degradation in the ^{3}sens* model systems for (A) azoxystrobin, (B) picoxystrobin, and (C) trifloxystrobin. Pesticide dissipation (top row) was biphasic and was plotted separately with the initial photoisomerization in the second row and the slower decay that followed shown in the third row. In the fourth row, the isomer formation is shown. It was assumed that the molar absorptivities of both the parent compound and isomer were equal in order to calculate the isomer formation relative to the parent compound initial concentration. The slopes of the lines obtained by linear regression and the coefficient of determination (R^2) are also included in the plots.

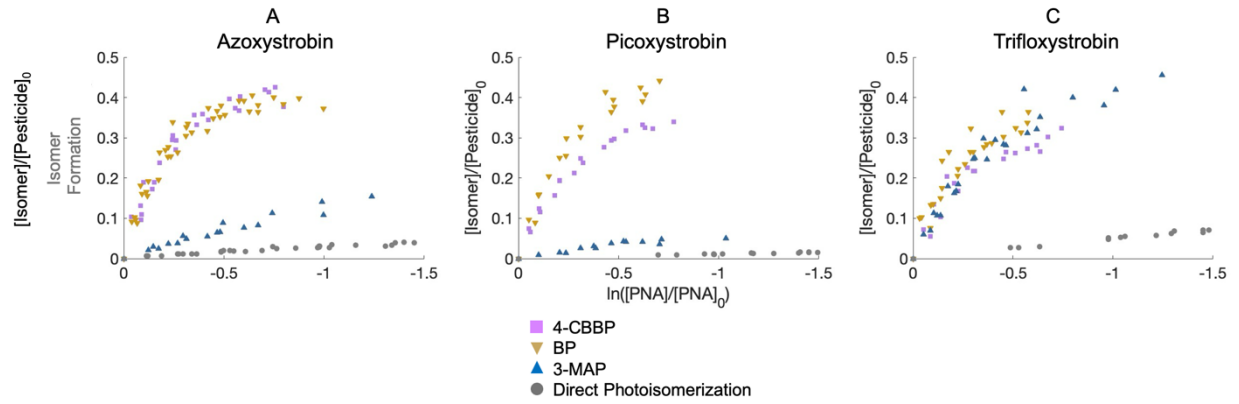

Figure S4.2. Isomer formation relative to the pesticide initial concentration plotted against PNA degradation for (A) azoxystrobin, (B) picoxystrobin, and (C) trifloxystrobin in the ^{3}sens* model systems and in direct photolysis control experiments. The molar absorptivities of the parent compound and isomer were assumed to be equal to calculate the isomer formation relative to the parent compound initial concentration.

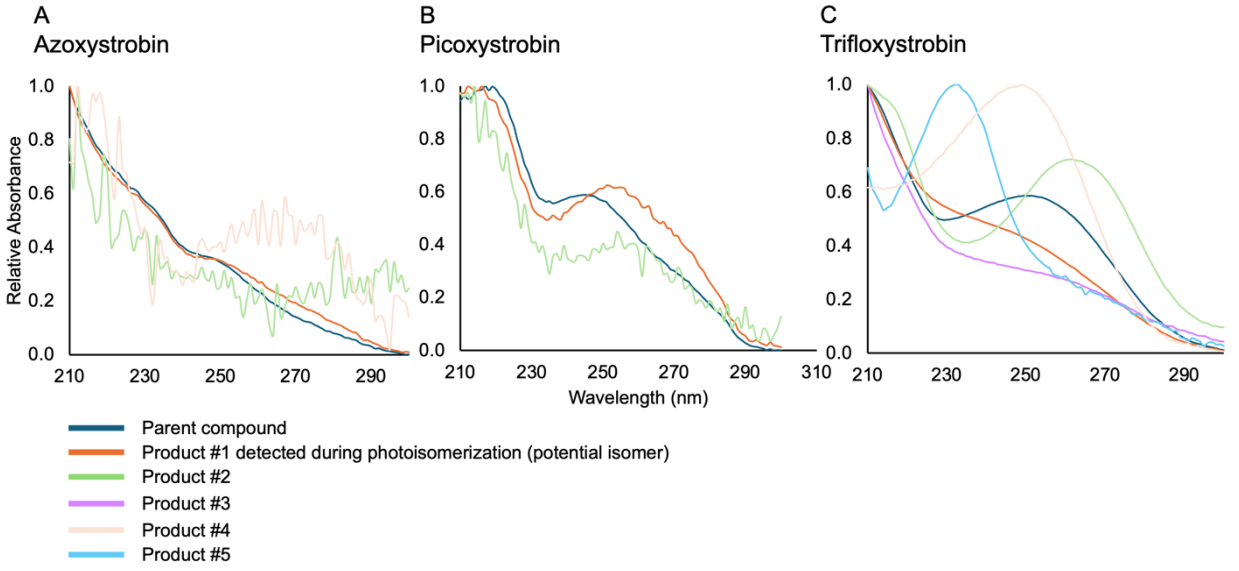

Figure S4.3. Relative absorbance of peaks detected during HPLC analysis for (A) azoxystrobin, (B) picoxystrobin, and (C) trifloxystrobin in ^{3}sens* model systems. The following wavelengths were used for quantitation for each parent compound and isomer: 235 nm for azoxystrobin, 265 nm for picoxystrobin, and 205 nm for trifloxystrobin (**Table S1.3**).

Table S4.1. Bimolecular reaction rate constants between ^{3}sens* and pesticides ($k_{^3sens^*}$, M^{-1} s^{-1}). When available, $k_{^3sens^*}$ reported in the literature were included for comparison to the values measured in this work. Plots of $k_{^3sens^*}$ obtained in this work and those available in the literature are also shown in **Figure S2.2**.

Pesticide	Bimolecular Reaction Rate Constant, $k_{^3sens^*}$ (M^{-1} s^{-1})			Literature (Sensitizer or ^{3}CDOM* Quencher)
	^{3}3-MAP*	^{3}4-CBBP*	^{3}BP*	
Acetochlor	$(8.17 \pm 0.42) \times 10^7$	$(7.17 \pm 0.62) \times 10^7$	$(2.57 \pm 0.13) \times 10^8$	HDA:[38] $(6.1\pm0.3)\times10^8$
Alachlor	$(1.93 \pm 0.13) \times 10^8$	$(8.26 \pm 0.63) \times 10^7$	$(3.73 \pm 0.21) \times 10^8$	HDA:[38] $(6.9\pm0.7)\times10^8$
Aminopyralid	n.a.[δ]	$(1.68 \pm 0.07) \times 10^8$	$(3.97 \pm 0.17) \times 10^8$	
Atrazine	n.a.[γ]	$(4.69 \pm 0.19) \times 10^8$	$(9.35 \pm 0.33) \times 10^8$	4-CBBP:[39] $(7.2\pm0.5)\times10^8$ CBBP:[39] 1.2×10^9 HDA:[38] $(1.2\pm0.2)\times10^9$
Azoxystrobin	[θ]$(3.68 \pm 0.23) \times 10^8$	$(3.81 \pm 0.25) \times 10^8$ [θ]$(1.24 \pm 0.08) \times 10^9$	$(3.89 \pm 0.70) \times 10^8$ [θ]$(3.86 \pm 0.32) \times 10^9$	
Chlorothalonil	$(1.05 \pm 0.04) \times 10^9$	$(2.03 \pm 0.11) \times 10^8$	$(3.43 \pm 0.11) \times 10^8$	
Chlorpyrifos	$(2.10 \pm 0.10) \times 10^8$	$(2.02 \pm 0.09) \times 10^8$	$(3.13 \pm 0.07) \times 10^8$	HDA:[38] $(2.7\pm1.3)\times10^7$
Cyproconazole	n.a.[γ]	n.a.[γ]	n.a.[γ]	
Cyprodinil	$(1.22 \pm 0.04) \times 10^9$	$(6.84 \pm 0.35) \times 10^8$	$(1.95 \pm 0.05) \times 10^9$	
Dicamba	$(1.36 \pm 0.09) \times 10^8$	$(4.61 \pm 0.35) \times 10^7$	$(1.75 \pm 0.10) \times 10^8$	
Difenoconazole	n.a.[γ]	$(3.27 \pm 0.25) \times 10^8$	$(4.08 \pm 0.28) \times 10^8$	
Fluroxypyr	$(1.19 \pm 0.06) \times 10^8$	$(4.57 \pm 0.24) \times 10^8$	$(1.50 \pm 0.06) \times 10^9$	
Fomesafen	$(1.24 \pm 0.04) \times 10^8$	$(3.67 \pm 0.17) \times 10^7$	$(4.10 \pm 0.11) \times 10^7$	
MCPA	$(1.51 \pm 0.09) \times 10^7$	$(2.33 \pm 0.08) \times 10^9$	$(7.87 \pm 0.20) \times 10^9$	
Mesotrione	$(8.83 \pm 0.51) \times 10^7$	$(3.47 \pm 0.16) \times 10^7$	$(3.68 \pm 0.21) \times 10^7$	HDA:[38] 7.80×10^8
Metconazole	$(1.36 \pm 0.11) \times 10^8$	$(9.83 \pm 0.77) \times 10^7$	$(4.37 \pm 0.29) \times 10^8$	
Metolachlor	$(1.05 \pm 0.07) \times 10^8$	$(7.41 \pm 0.56) \times 10^7$	n.a.[γ]	HDA:[38] $(9.8\pm1.7)\times10^8$
Pendimethalin	$(2.22 \pm 0.11) \times 10^8$	$(8.50 \pm 0.35) \times 10^7$	$(1.37 \pm 0.03) \times 10^8$	
Picloram	$(2.26 \pm 0.16) \times 10^8$	$(1.51 \pm 0.06) \times 10^8$	$(2.02 \pm 0.09) \times 10^9$	
Picoxystrobin	n.a.[γ]	$(3.48 \pm 0.37) \times 10^8$ [θ]$(1.12 \pm 0.05) \times 10^9$	$(8.06 \pm 0.36) \times 10^8$ [θ]$(2.31 \pm 0.11) \times 10^9$	
Propiconazole	n.a.[γ]	n.a.[γ]	n.a.[γ]	HDA:[38] $(1.3\pm0.4)\times10^8$
Prothioconazole (pH=5)	$(1.71 \pm 0.05) \times 10^9$	$(9.51 \pm 0.33) \times 10^8$	$(2.15 \pm 0.05) \times 10^9$	
Prothioconazole (pH=9)	$(8.22 \pm 0.26) \times 10^8$	$(4.51 \pm 0.16) \times 10^8$	$(9.49 \pm 0.27) \times 10^8$	
Pyraclostrobin	n.a.[δ]	n.a.[δ]	n.a.[δ]	
Pyrimethanil	$(9.75 \pm 0.36) \times 10^8$	$(9.26 \pm 0.38) \times 10^8$	$(1.47 \pm 0.04) \times 10^9$	

Table S4.1. Continued

Pesticide	Bimolecular Reaction Rate Constant, k^{3}_{sens*} (M^{-1} s^{-1})			Literature (Sensitizer or ^{3}CDOM* Quencher)
	^{3}3-MAP*	^{3}4-CBBP*	^{3}BP*	
Tebuconazole	$(5.08 \pm 0.37) \times 10^{7}$	$(9.75 \pm 0.55) \times 10^{7}$	$(1.39 \pm 0.07) \times 10^{8}$	4-CBBP:[33] $(2.5 \pm 0.1) \times 10^{8}$
Thiobencarb	$(1.11 \pm 0.07) \times 10^{8}$	$(1.68 \pm 0.07) \times 10^{8}$	$(2.14 \pm 0.07) \times 10^{8}$	
Triclopyr	n.a.$^{\delta}$	$(1.38 \pm 0.07) \times 10^{8}$	$(6.12 \pm 0.27) \times 10^{8}$	
Trifloxystrobin	$(7.06 \pm 0.48) \times 10^{8}$ $^{\theta}(2.26 \pm 0.07) \times 10^{9}$	$(6.69 \pm 0.80) \times 10^{8}$ $^{\theta}(1.73 \pm 0.06) \times 10^{9}$	$(1.15 \pm 0.13) \times 10^{9}$ $^{\theta}(3.62 \pm 0.24) \times 10^{9}$	

$^{\delta}$ *Only direct photolysis was observed.*

$^{\gamma}$ *No degradation of the pesticide was observed in the model system.*

$^{\theta}$ *Photoisomerization bimolecular reaction rate constant.*

HDA = trans,trans-hexadienoic acid

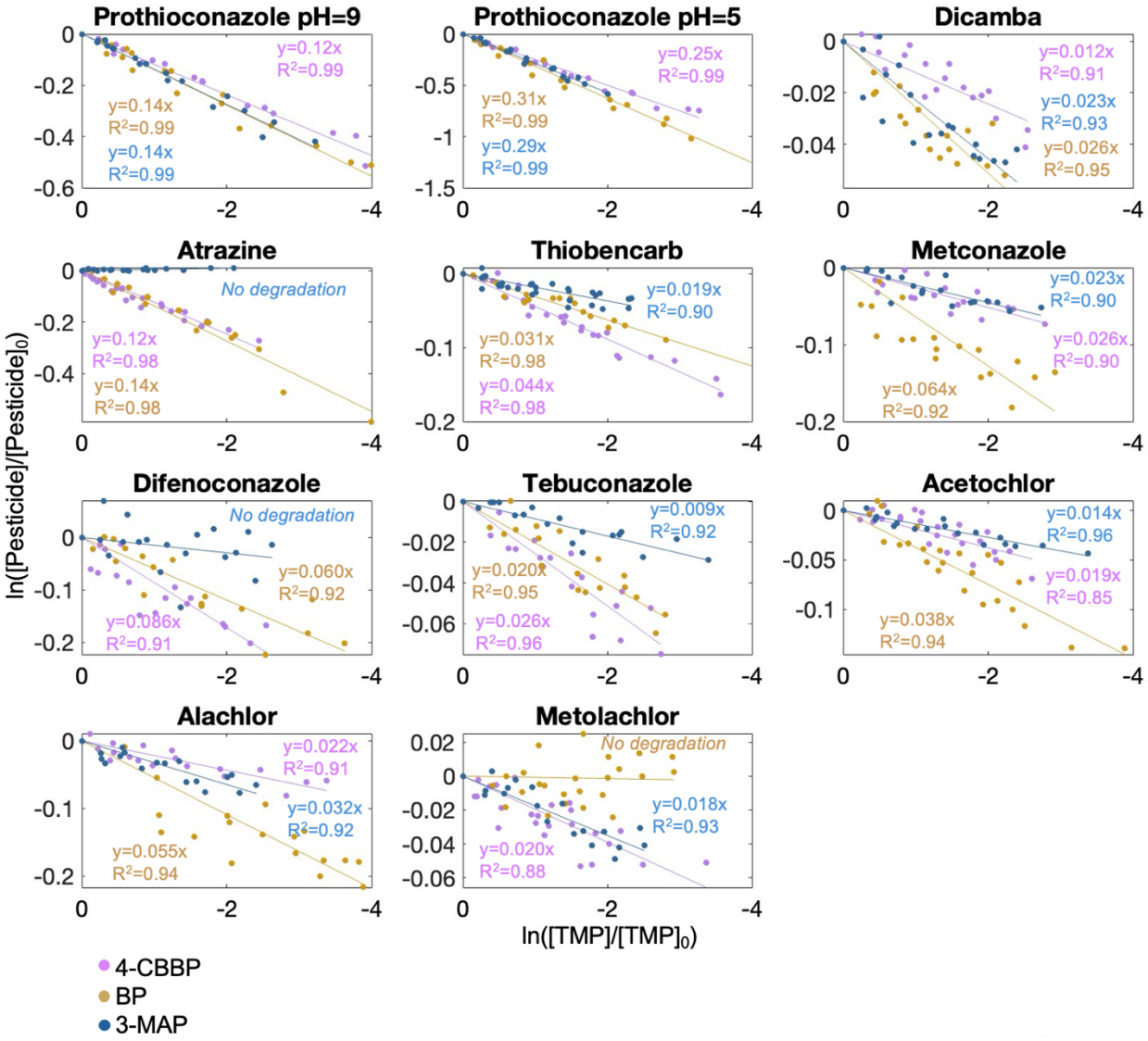

Figure S4.4. Observed degradation of the pesticides plotted against TMP degradation using BP, 4-CBBP, or 3-MAP as the sensitizers. Photodegradation of pesticides that underwent photoisomerization were plotted in **Figure S4.5**. For pesticides that degraded in direct photolysis control experiments, the observed degradation of the pesticide was plotted against PNA degradation in **Figure S4.6**. When TMP as the probe compound affected observed degradation rates, the degradation of the pesticide was plotted against PNA degradation in **Figure S4.7**. For pesticides that did not degrade in any ^{3}sens* model system, plots are shown in **Figure S4.8**.

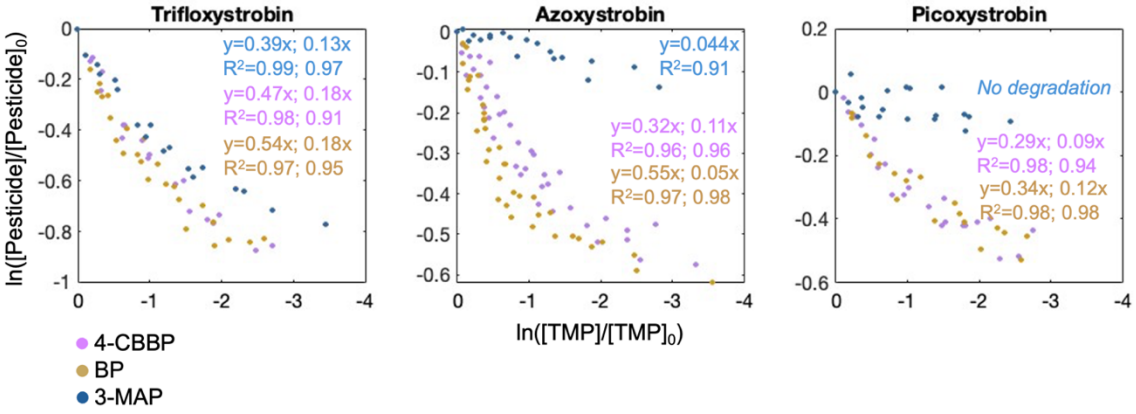

Figure S4.5. Observed degradation of the pesticides that had a biphasic decay plotted against TMP degradation in experiments with 4-CBBP (pink), BP (yellow), or 3-MAP (blue) as the sensitizers.

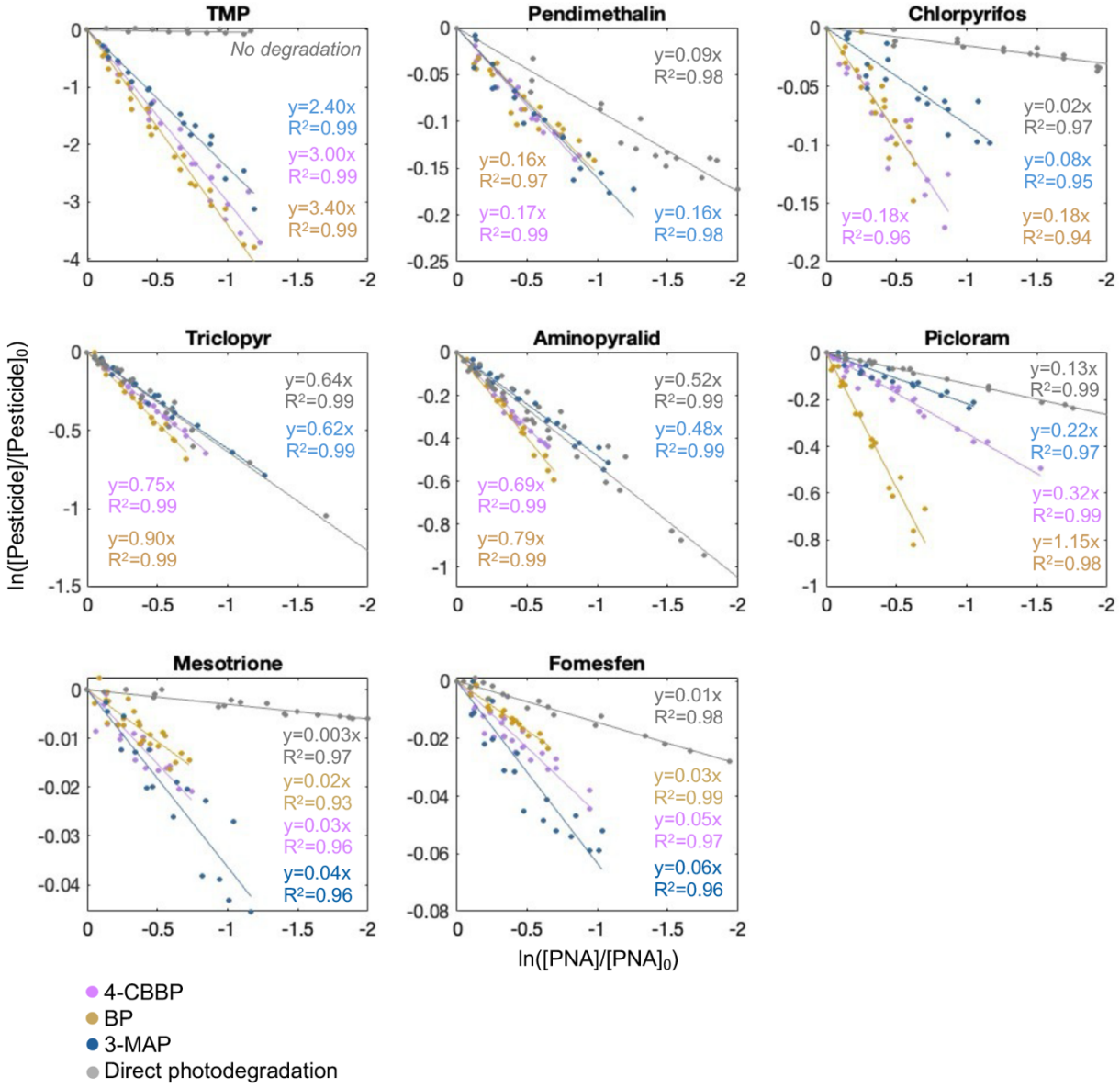

Figure S4.6. Observed degradation of pesticides that degraded in direct photolysis control experiments plotted against PNA degradation in experiments using 4-CBBP (pink), BP (yellow), or 3-MAP (blue) as the sensitizers and in the direct photolysis control experiments (grey).

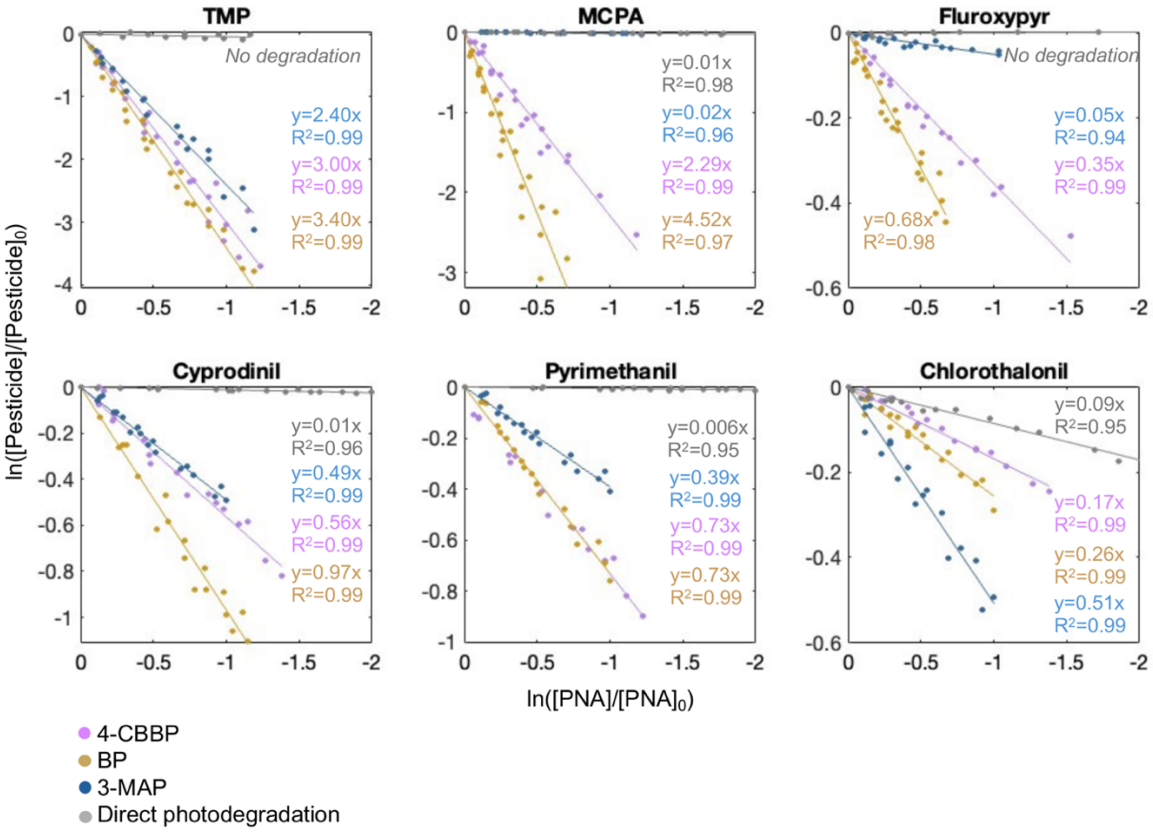

Figure S4.7. Observed degradation of pesticides that had degradation rates influenced by the presence of TMP as the probe compound plotted against PNA degradation in experiments using 4-CBBP (pink), BP (yellow), or 3-MAP (blue) as the sensitizer and in the direct photolysis control experiments (grey).

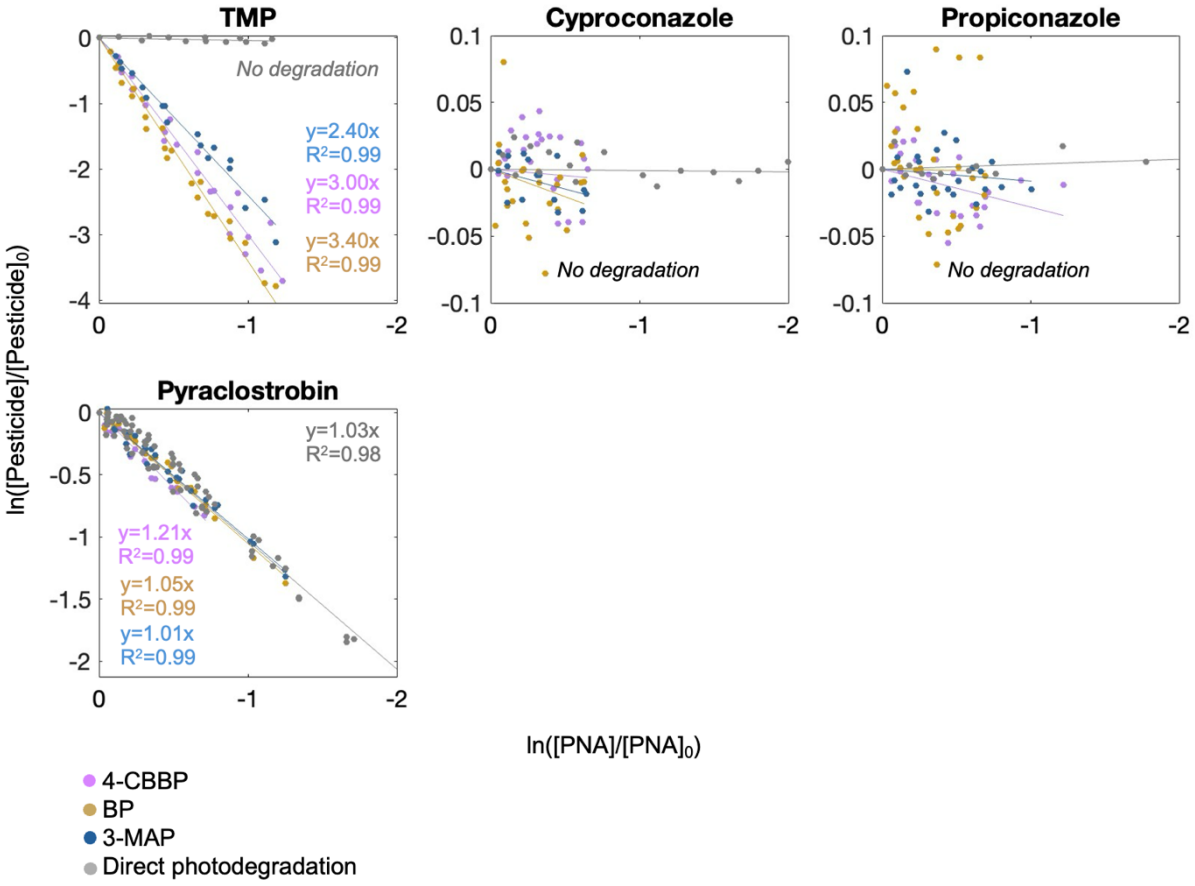

Figure S4.8. Observed degradation of pesticides that did not degrade in any of the ^{3}sens* model systems plotted against PNA degradation in experiments using 4-CBBP (pink), BP (yellow), or 3-MAP (blue) as the sensitizer and in the direct photolysis control experiments (grey).

A

Chloroacetamide herbicides

(*Contain aniline substructures*)

Acetochlor

k^{3}4-CBBP*,i =(1.4±0.3)×10^{8} M^{-1} s^{-1}

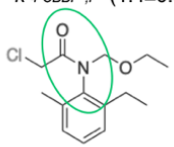

Alachlor

k^{3}4-CBBP*,i =(1.6±0.4)×10^{8} M^{-1} s^{-1}

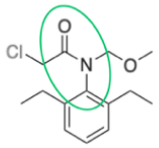

Metolachlor

k^{3}4-CBBP*,i =(1.5±0.3)×10^{8} M^{-1} s^{-1}

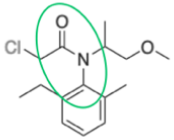

B

Amino-substituted aromatic heterocycles

Aminopyralid

k^{3}4-CBBP*,i =(3.3±0.7)×10^{8} M^{-1} s^{-1}

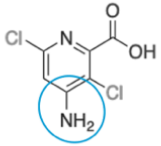

Fluroxypyr

k^{3}4-CBBP*,i =(9.0±2.0)×10^{8} M^{-1} s^{-1}

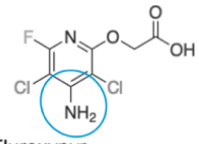

Picloram

k^{3}4-CBBP*,i =(3.0±0.7)×10^{8} M^{-1} s^{-1}

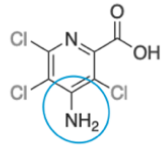

Cyprodinil

k^{3}4-CBBP*,i =(1.4±0.3)×10^{9} M^{-1} s^{-1}

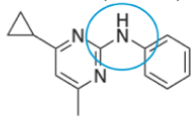

Pyrimethanil

k^{3}4-CBBP*,i =(1.8±0.4)×10^{9} M^{-1} s^{-1}

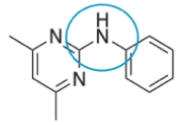

Atrazine

k^{3}4-CBBP*,i =(9.2±0.2)×10^{8} M^{-1} s^{-1}

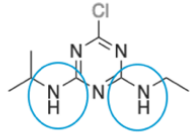

Pendimethalin

k^{3}4-CBBP*,i =(1.7±0.4)×10^{8} M^{-1} s^{-1}

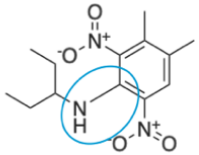

C

Sulfur-containing compounds

Prothioconazole

k^{3}4-CBBP*,i =(1.9±0.4)×10^{9} M^{-1} s^{-1} (pH=5)

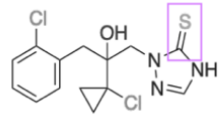

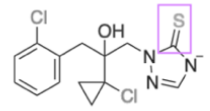

k^{3}4-CBBP*,i =(8.9±1.9)×10^{8} M^{-1} s^{-1} (pH=9)

Chlorpyrifos

k^{3}4-CBBP*,i =(4.0±0.9)×10^{8} M^{-1} s^{-1}

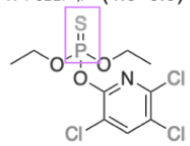

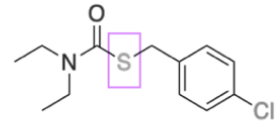

Thiobencarb

k^{3}4-CBBP*,i =(3.3±0.7)×10^{8} M^{-1} s^{-1}

Fomesafen

k^{3}4-CBBP*,i =(7.2±1.6)×10^{7} M^{-1} s^{-1}

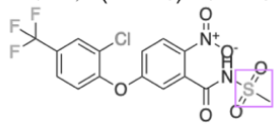

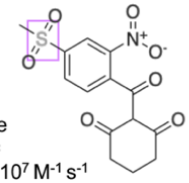

Mesotrione

k^{3}4-CBBP*,i =

(6.8±1.5)×10^{7} M^{-1} s^{-1}

Figure S4.9. Continued.

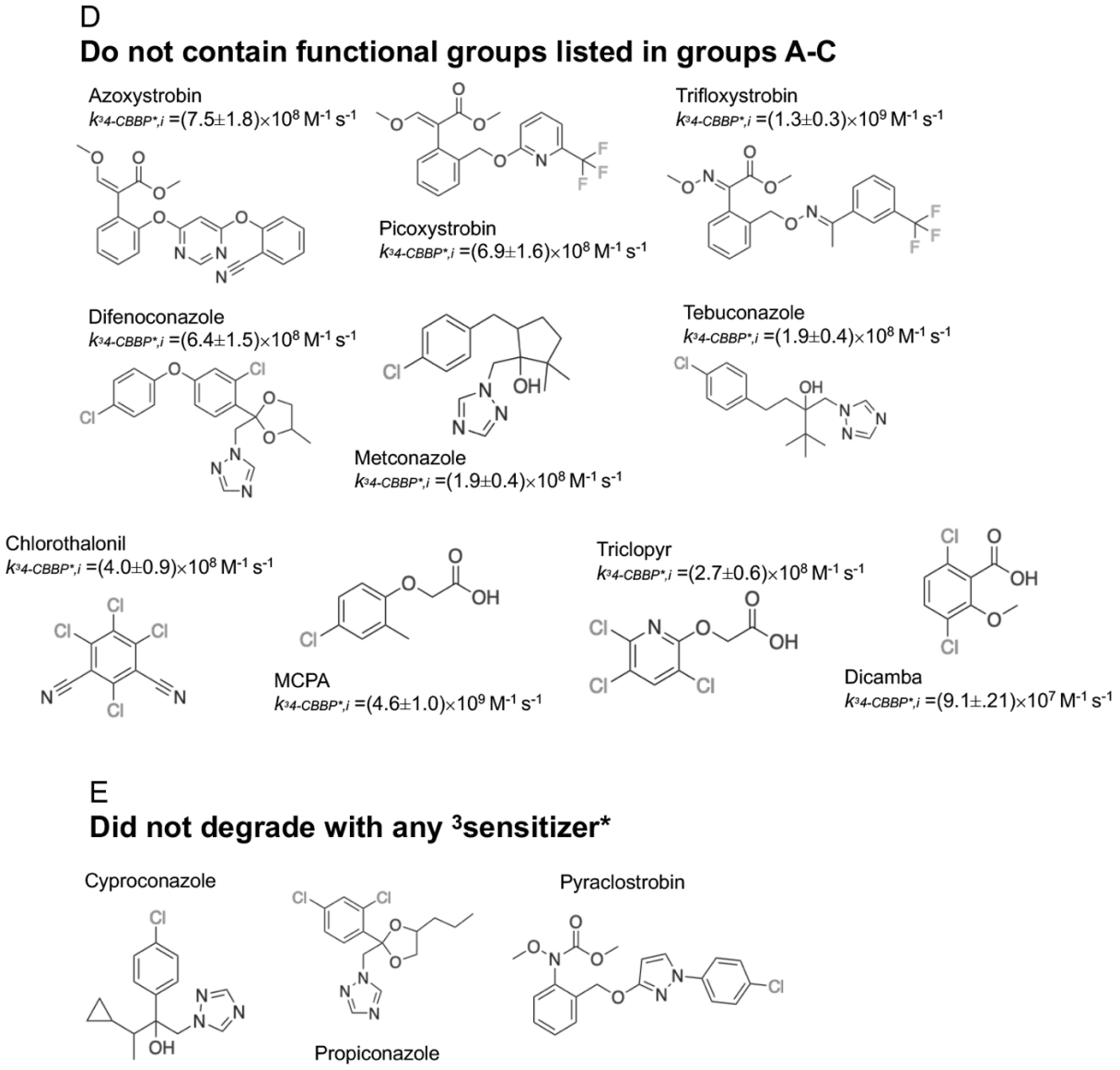

Figure S4.9. Structures of pesticides that degraded with ^{3}sens* (A-D) or did not degrade in the ^{3}sens* model systems (E). The A-C groups include pesticides that contain (A) aniline substructures (chloroacetamide herbicides), (B) amino-substituted aromatic heterocycles, or (C) sulfur atoms. These functional groups were previously identified as susceptible to reactions with ^{3}CDOM*.[37] Group D contains the remaining pesticides that degraded with ^{3}sens* but did not contain any of these functional groups. The k^{3}*4-CBBP** of these pesticides were included for comparison of the values measured for each pesticide (**Table S4.1**).

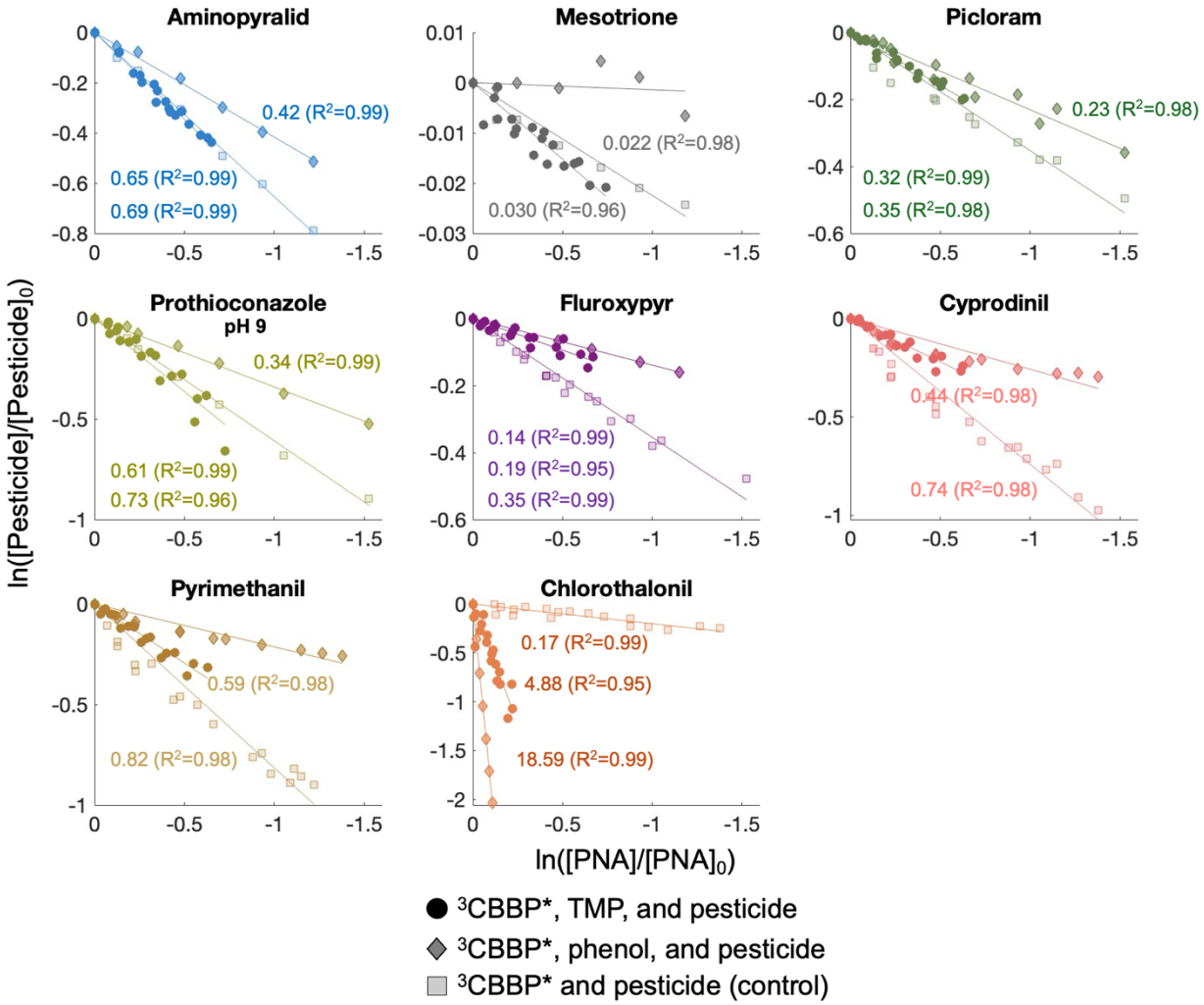

Figure S4.10. Degradation of the pesticide plotted against PNA degradation in experiments evaluating pesticide susceptibility to back-reactions using phenol as a model antioxidant. Data for pesticides that showed differences in degradation rates with and without phenol addition are included. Three experimental scenarios were compared: (1) pesticide degradation using 4-CBBP as the sensitizer and TMP as the probe compound, (2) pesticide degradation including the addition of 10 μM phenol as a model antioxidant, and (3) a control experiment without the addition of TMP or phenol. Data for MCPA (with 4-CBBP and 3-MAP as ^{3}sens*) are presented in **Figure S4.11**. Data for pesticides that had similar degradation rates in all conditions are shown in **Figure S4.12**.

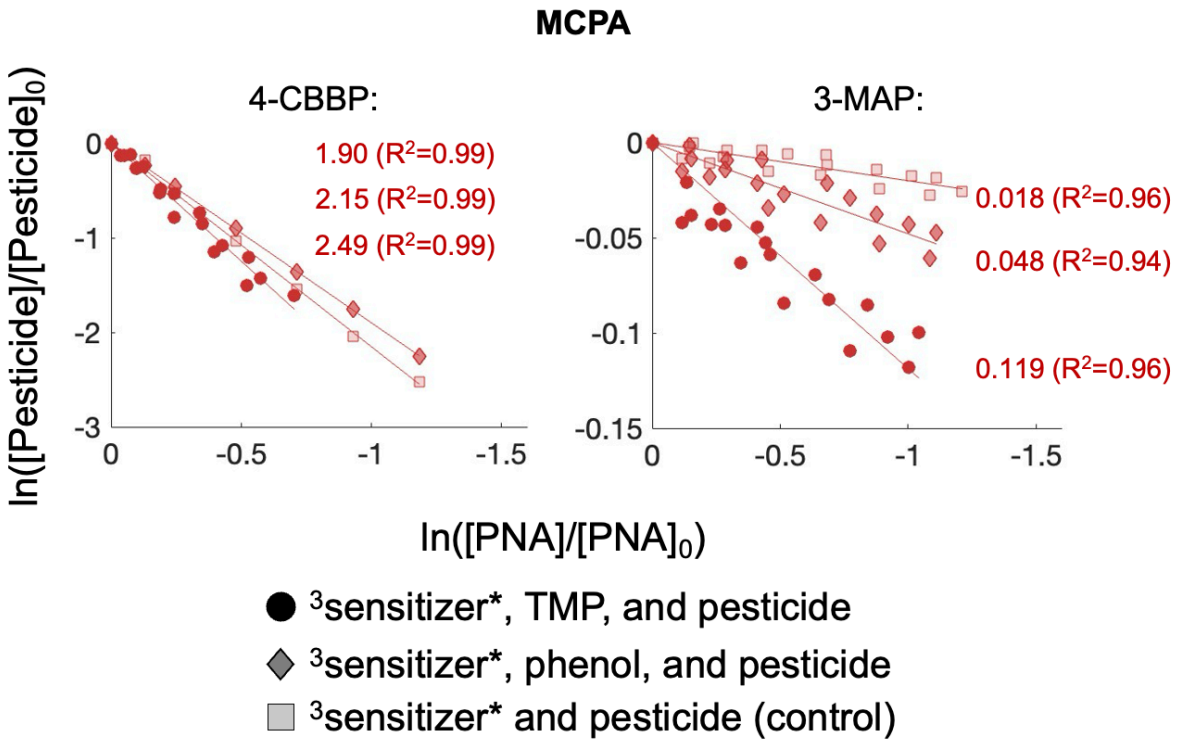

Figure S4.11. Degradation of MCPA plotted against PNA degradation in experiments using either 4-CBBP or 3-MAP as the sensitizer to evaluate pesticide susceptibility to back-reactions with a model antioxidant (phenol). Three experimental scenarios were compared: (1) pesticide degradation using 4-CBBP as the sensitizer and TMP as the probe compound, (2) pesticide degradation including the addition of 10 µM phenol as a model antioxidant, and (3) a control experiment without the addition of TMP or phenol.

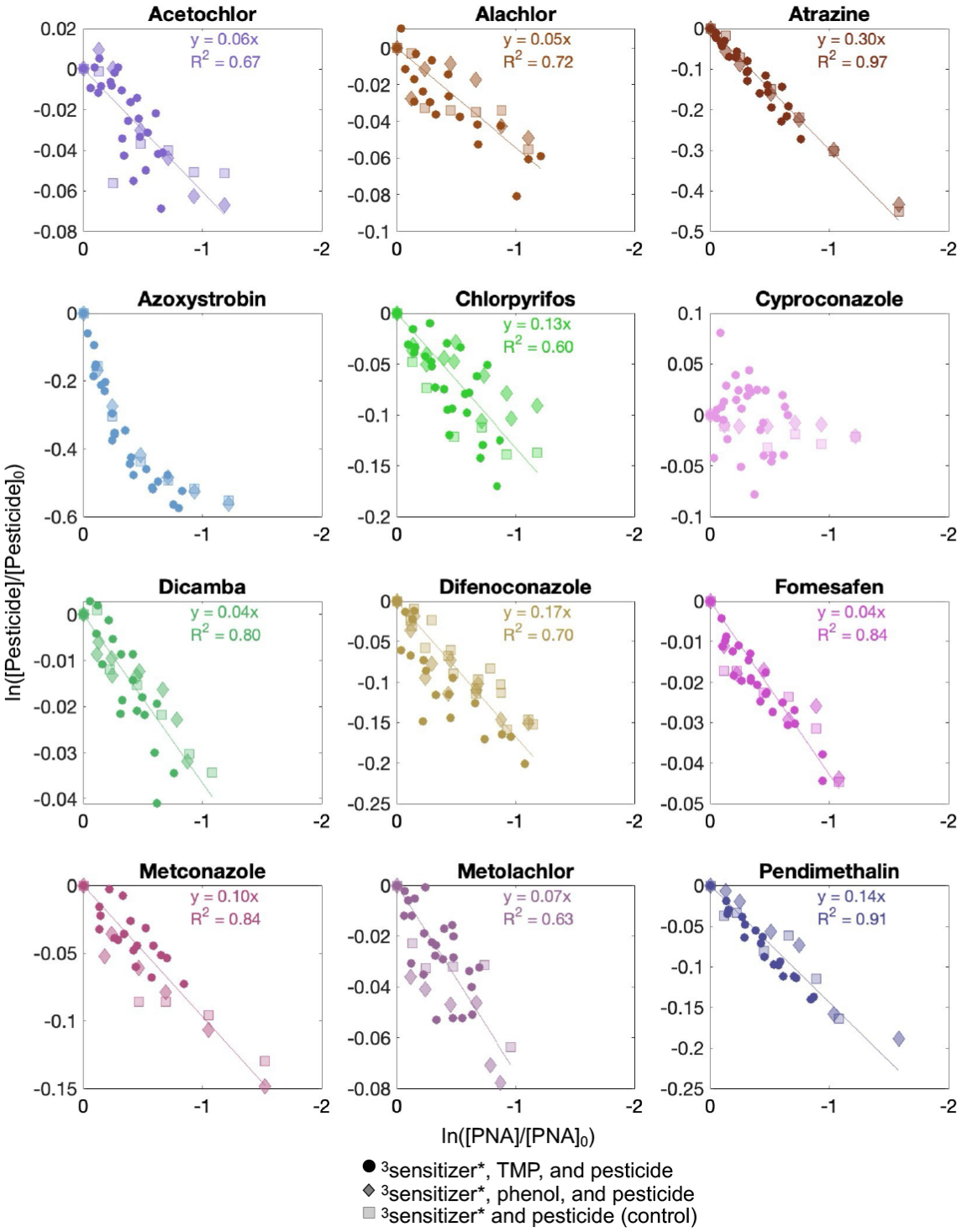
Acetochlor
y = 0.06x
R2 = 0.67
Alachlor
y = 0.05x
R2 = 0.72
Atrazine
y = 0.30x
R2 = 0.97
Azoxystrobin
Chlorpyrifos
y = 0.13x
R2 = 0.60
Cyproconazole
Dicamba
y = 0.04x
R2 = 0.80
Difenoconazole
y = 0.17x
R2 = 0.70
Fomesafen
y = 0.04x
R2 = 0.84
Metconazole
y = 0.10x
R2 = 0.84
Metolachlor
y = 0.07x
R2 = 0.63
Pendimethalin
y = 0.14x
R2 = 0.91
ln([Pesticide]/[Pesticide]0)
ln([PNA]/[PNA]0)
3sensitizer*, TMP, and pesticide
3sensitizer*, phenol, and pesticide
3sensitizer* and pesticide (control)

Figure S4.12. Continued.

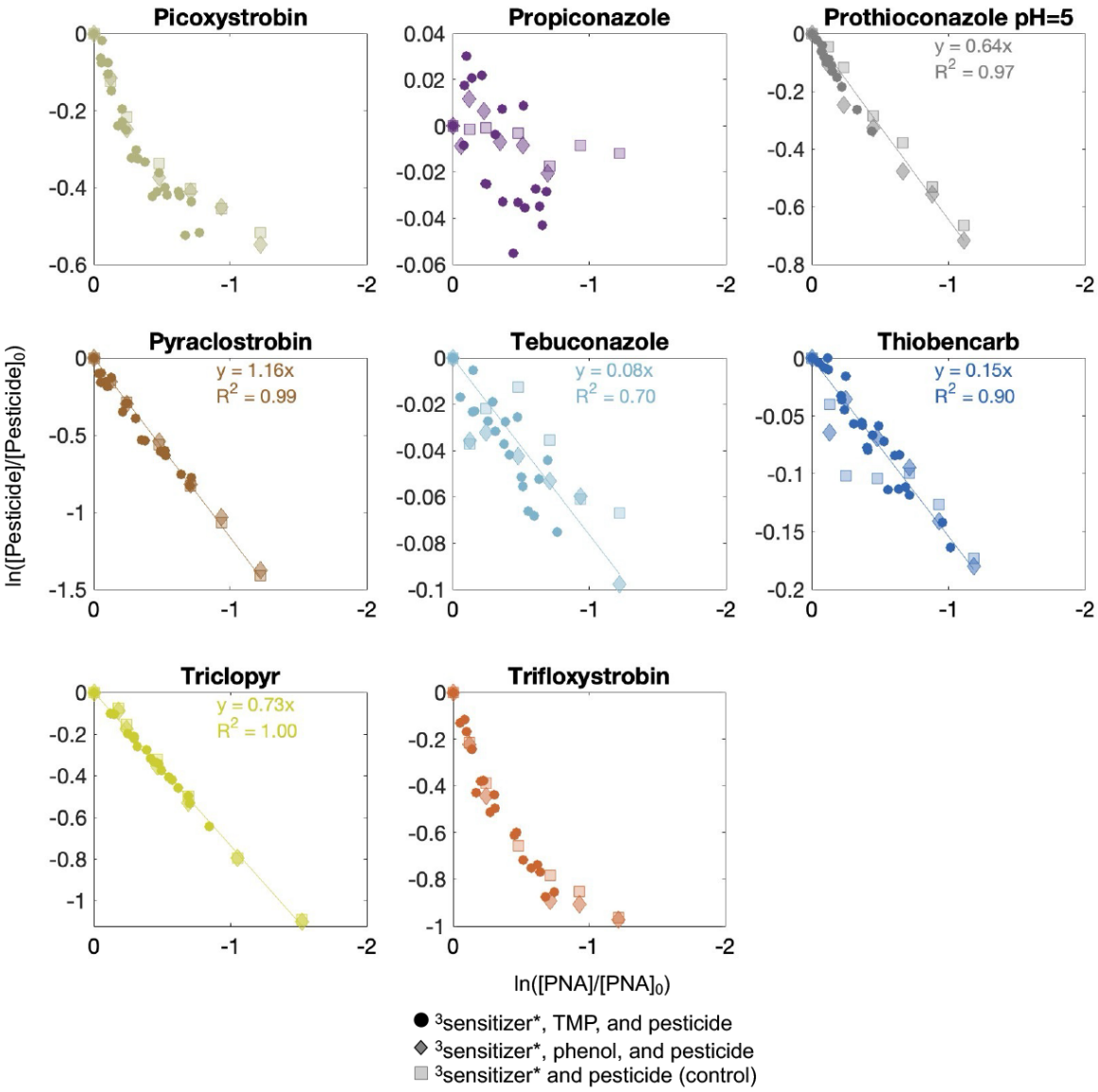

Figure S4.12. Degradation of the pesticide plotted against PNA degradation for pesticides that showed similar degradation rates with or without the addition of phenol as a model antioxidant. Three experimental scenarios were compared: (1) pesticide degradation using 4-CBBP as the sensitizer and TMP as the probe compound, (2) pesticide degradation including the addition of 10 μM phenol as a model antioxidant, and (3) a control experiment without the addition of TMP or phenol.

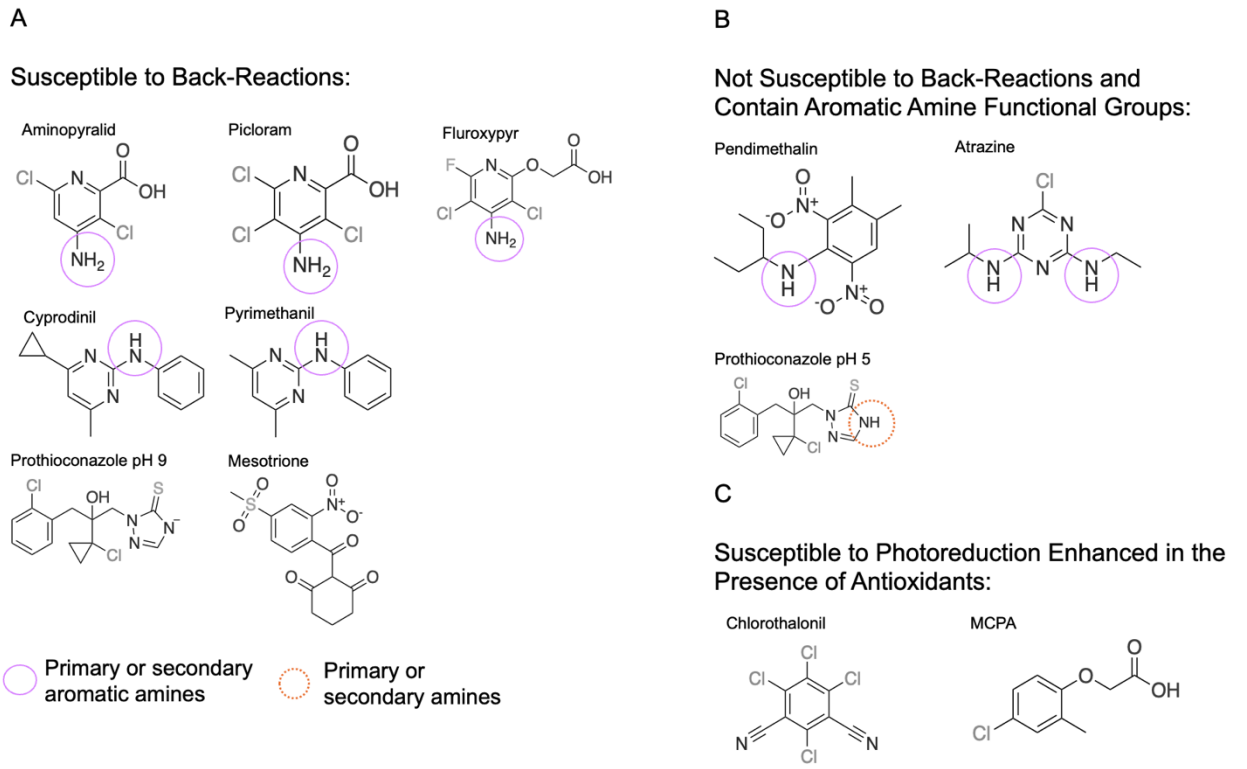

Figure S4.13. Pesticides that were (A) susceptible to back-reactions in the presence of phenol as a model antioxidant using 4-CBBP as the sensitizer, (B) not susceptible to back-reactions but contain amine and/or aromatic amine functional groups, and (C) susceptible to photoreduction accelerated in the presence of antioxidants (for MCPA, this was only observed when using 3-MAP as the sensitizer).

REFERENCES

1. J. Wenk and S. Canonica, Phenolic antioxidants inhibit the triplet-induced transformation of anilines and sulfonamide antibiotics in aqueous solution, *Environ Sci Technol*, 2012, **46**, 5455-5462.
2. J. N. Apell, S. Kliegman, C. Sola-Gutierrez and K. McNeill, Linking Triclosan's Structural Features to Its Environmental Fate and Photoproducts, *Environ Sci Technol*, 2020, **54**, 14432-14441.
3. S. Canonica, B. Hellrung and J. Wirz, Oxidation of Phenols by Triplet Aromatic Ketones in Aqueous Solution, *J. Phys. Chem. A*, 2000, **104**, 1226-1232.
4. M. Minella, L. Rapa, L. Carena, M. Pazzi, V. Maurino, C. Minero, M. Brigante and D. Vione, An experimental methodology to measure the reaction rate constants of processes sensitised by the triplet state of 4-carboxybenzophenone as a proxy of the triplet states of chromophoric dissolved organic matter, under steady-state irradiation conditions, *Environ Sci Process Impacts*, 2018, **20**, 1007-1019.
5. A. A. Lamola and G. S. Hammond, Mechanisms of Photochemical Reactions in Solution. XXXIII. Intersystem Crossing Efficiencies, *The Journal of Chemical Physics*, 1965, **43**, 2129-2135.
6. J. K. Hurley, H. Linschitz and A. Treinin, Interaction of Halide and Pseudohalide Ions with Triplet Benzophenone-4-carboxylate: Kinetics and Radical Yields, *J. Phys. Chem.*, 1988, **92**, 5151-5159.
7. L. de Brito Anton, A. I. Silverman and J. N. Apell, Determining wavelength-dependent quantum yields of photodegradation: importance of experimental setup and reference values for actinometers, *Environ Sci Process Impacts*, 2024, **26**, 1052-1063.
8. T. Arakaki, T. Miyake, T. Hirakawa and H. Sakugawa, pH Dependent Photoformation of Hydroxyl Radical and Absorbance of Aqueous-Phase N(III) (HNO2 and NO2-), *Environ Sci Technol*, 1999, **33**, 2561-2565.
9. L. Chu and C. Anastasio, Formation of Hydroxyl Radical from the Photolysis of Frozen Hydrogen Peroxide, *J Phys Chem A*, 2005, **109**, 6264-6271.
10. J. L. Acero, F. J. Benitez, F. J. Real and C. Maya, Oxidation of Acetamide Herbicides in Natural Waters by Ozone and by the Combination of Ozone/Hydrogen Peroxide: Kinetic Study and Process Modeling, *Ind. Eng. Chem. Res.*, 2003, **42**, 5762-5769.
11. J. F. Brekken and P. L. Brezonik, Indirect Photolysis of Acetochlor: Rate Constant of a Nitrate-Mediated Hydroxyl Radical Reaction, *Chemosphere*, 1998, **36**, 2699-2704.
12. W. Song, V. Ravindran and M. Pirbazari, Process optimization using a kinetic model for the ultraviolet radiation-hydrogen peroxide decomposition of natural and synthetic organic compounds in groundwater, *Chemical Engineering Science*, 2008, **63**, 3249-3270.
13. J. De Laat, P. Maouala-Makata and M. Dore, Constantes Cinetiques de Reaction de L'Ozone Moleculaire et des Radicaux Hydroxyles Sur Quelques Phenyl-Urees et Acetamides Rate Constants for Reactions of Ozone and Hydroxyl Radicals with Several Phenyl-Ureas and Acetamides, *Environmental Technology*, 1996, **17**, 707-716.
14. S. Sanches, M. T. Barreto Crespo and V. J. Pereira, Drinking water treatment of priority pesticides using low pressure UV photolysis and advanced oxidation processes, *Water Res*, 2010, **44**, 1809-1818.
15. W. R. Haag and C. C. D. Yao, Rate Constants for Reaction of Hydroxyl Radicals with Several Drinking Water Contaminants, *Environ Sci Technol*, 1992, **26**, 1005-1013.

16. S. A. Mabury and D. G. Crosby, Pesticide Reactivity toward Hydroxyl and Its Relationship to Field Persistence, *J. Agric. Food Chem.*, 1996, **44**, 1920-1924.
17. N. Chramosta, J. De Laat, M. Dore, H. Suty and M. Pouillot, Determination des constantes cinetiques de reaction des radicaux hydroxyles sur quelques s-triazines, *Environmental Technology*, 1993, **14**, 215-226.
18. J. De Laat, M. Doré and H. Suty, Oxydation de S-triazines par les procédés d'oxydation radicalaire. Sous-produits de réaction et constantes cinétiques de réaction, *Revue des sciences de l'eau*, 1995, **8**, 23-42.
19. M. E. Azenha, H. D. Burrows, M. Canle, R. Coimbra, M. I. Fernandez, M. V. Garcia, A. E. Rodrigues, J. A. Santaballa and S. Steenken, On the kinetics and energetics of one-electron oxidation of 1,3,5-triazines, *Chem Commun (Camb)*, 2003, DOI: 10.1039/b210119j, 112-113.
20. B. Balci, N. Oturan, R. Cherrier and M. A. Oturan, Degradation of atrazine in aqueous medium by electrocatalytically generated hydroxyl radicals. A kinetic and mechanistic study, *Water Res*, 2009, **43**, 1924-1934.
21. J. L. Acero, K. Stemmler and U. von Guten, Degradation Kinetics of Atrazine and Its Degradation Products with Ozone and OH Radicals: A Predictive Tool for Drinking Water Treatment, *Environ Sci Technol*, 2000, **34**, 591-597.
22. A. Tauber and C. von Sonntag, Products and Kinetics of the OH-radical-induced Dealkylation of Atrazine, *Acta Hydrocim. Hydrobiol.*, 2000, **28**, 15-23.
23. F. J. Beltran, G. Ovejero and B. Acedo, Oxidation of Atrazine in Water by Ultraviolet Radiation Combined with Hydrogen Peroxide, *Water Res*, 1993, **27**, 1013-1021.
24. K. L. Armbrust, Pesticide hydroxyl radical rate constants: Measurements and estimates of their importance in aquatic environments, *Environmental Toxicology and Chemistry*, 2009, **19**, 2175-2180.
25. C. Wu, H. Shemer and K. G. Linden, Photodegradation of Metolachlor Applying UV and UV/H2O2, *J. Agric. Food Chem.*, 2007, **55**, 4059-4065.
26. A. P. Bhat, W. C. K. Pomerantz and W. A. Arnold, Finding Fluorine: Photoproduct Formation during the Photolysis of Fluorinated Pesticides, *Environ Sci Technol*, 2022, **56**, 12336-12346.
27. F. Fdil, J. J. Aaron, N. Oturan, A. Chaouch and M. A. Oturan, Dégradation photochimique d'herbicides chlorophenoxyalcanoïques en milieux aqueux, *Revue des sciences de l'eau*, 2005, **16**, 123-142.
28. F. J. Benitez, J. L. Acero, F. J. Real and S. Roman, Oxidation of MCPA and 2,4-D by UV radiation, ozone, and the combinations UV/H2O2 and O3/H2O2, *J Environ Sci Health B*, 2004, **39**, 393-409.
29. F. Al Housari, P. Hohener and S. Chiron, Factors responsible for rapid dissipation of acidic herbicides in the coastal lagoons of the Camargue (Rhone River Delta, France), *Sci Total Environ*, 2011, **409**, 582-587.
30. M. Murati, N. Oturan, J. J. Aaron, A. Dirany, B. Tassin, Z. Zdravkovski and M. A. Oturan, Degradation and mineralization of sulcotrione and mesotrione in aqueous medium by the electro-Fenton process: a kinetic study, *Environ Sci Pollut Res Int*, 2012, **19**, 1563-1573.
31. N. Bensalah, A. Khodary and A. Abdel-Wahab, Kinetic and mechanistic investigations of mesotrione degradation in aqueous medium by Fenton process, *J Hazard Mater*, 2011, **189**, 479-485.

32. S. Huntscha, H. Singer, S. Canonica, R. P. Schwarzenbach and K. Fenner, Input Dynamic and Fate in Surface Water of the Herbicide Metolachlor and of its Highly Mobile Transformation Product Metolachlor ESA, *Environ Sci Technol*, 2008, **42**, 5507-5513.
33. L. Carena, A. Scozzaro, M. Romagnoli, M. Pazzi, L. Martone, C. Minero, M. Minella and D. Vione, Phototransformation of the fungicide tebuconazole, and its predicted fate in sunlit surface freshwaters, *Chemosphere*, 2022, **303**, 134895.
34. C. A. Davis, K. McNeill and E. M. Janssen, Non-Singlet Oxygen Kinetic Solvent Isotope Effects in Aquatic Photochemistry, *Environ Sci Technol*, 2018, **52**, 9908-9916.
35. M. A. Malouki, L. Cavani, A. ter Halle, C. Ciavatta and C. Richard, Photosensitizing properties of formulation adjuvants, *Journal of Photochemistry and Photobiology A: Chemistry*, 2009, **203**, 186-191.
36. A. ter Halle and C. Richard, Simulated Solar Light Irradiation of Meostrione in Natural Waters, *Environ Sci Technol*, 2006, **40**, 3842-3847.
37. K. McNeill and S. Canonica, Triplet state dissolved organic matter in aquatic photochemistry: reaction mechanisms, substrate scope, and photophysical properties, *Environ Sci Process Impacts*, 2016, **18**, 1381-1399.
38. T. Zeng and W. A. Arnold, Pesticide photolysis in prairie potholes: probing photosensitized processes, *Environ Sci Technol*, 2013, **47**, 6735-6745.
39. L. Carena, C. G. Puscasu, S. Comis, M. Sarakha and D. Vione, Environmental photodegradation of emerging contaminants: A re-examination of the importance of triplet-sensitised processes, based on the use of 4-carboxybenzophenone as proxy for the chromophoric dissolved organic matter, *Chemosphere*, 2019, **237**, 124476.